國立交通大學

電機學院與資訊學院 電信學程

碩 士 論 文

Ka 頻段中繼雙訊模組設計

Design of a Ka band HUB diplexer module

研 究 生：歐宗信

指導教授：鍾世忠 教授

中 華 民 國 九 十 五 年 九 月

Ka 頻段中繼雙訊模組設計
Design of a Ka band HUB diplexer module

研 究 生：歐宗信　　Student：Tsung-Hsing Ou

指導教授：鍾世忠　　Advisor：Dr. Shyh-Jong Chung

國 立 交 通 大 學

電機學院與資訊學院專班 電信學程

碩 士 論 文

A Thesis

Submitted to Degree Program of Electrical Engineering and Computer Science

College of Electrical and Computer Engineering

National Chiao Tung University

in Partial Fulfillment of the Requirements

for the Degree of

Master of Science

in

Communication Engineering

September 2006

Hsinchu, Taiwan, Republic of China

中華民國九十五年九月

Ka 頻段中繼雙訊模組設計

學生：歐宗信　　指導教授：鍾世忠 教授

國立交通大學 電機學院與資訊學院 電信學程（研究所）碩士班

摘　　要

本論文研製之 Ka 頻段中繼雙訊模組設計，可應用於智慧型傳輸系統(ITS, Intelligent Transport System)中，扮演車置單元(OBU, On-board Unit)或是車道單元(RSU, Road-side Unit)的角色。其不僅是一個微波頻段(中頻信號)與微米波頻段(射頻信號)昇、降頻的介面，也允許提供全雙工的傳輸通道給予其工作頻段接近 2.4GHz 的單元 A 與 B(ELEMENT A and B)。

此模組包括三個子模組：中頻子模組、本地頻率子模組與射頻子模組。中頻子模組的功能是將單元 A 的工作頻段昇頻至 3.4GHz，並將其與單元 B 信號合成為中頻信號。本地頻率子模組含有一個壓控震盪器與鎖相迴路電路，穩定地提供不僅一組 5.85GHz 的本地信號源給中頻子模組，且利用三倍頻器、功率分配器與放大器產生額外兩組 17.55Ghz 本地信號源給發射與接收之射頻子模組。射頻子模組利用內部的次諧波混頻器電路，將中頻信號昇頻至射頻頻段並藉由天線發射，或是將接收到的射頻信號降頻至中頻頻段給中頻子模組。

最後量測的結果是:車置單元與車道單元之間的傳送距離為 10 公尺於資料傳輸率為每秒 950 千位元時。

Design of a Ka band HUB diplexer module

Student：Tsung-Hsing Ou Advisors：Dr. Shyh-Jong Chung

Degrees Program of Electrical Engineering Computer Science
National Chiao Tung University

ABSTRACT

The thesis is a design of Ka band HUB diplexer module which would be applied to the intelligent transport system to play the role of on-board or road-side unit. It is not only the interface between the microwave (IF signal) and millimeter-wave (RF signal) to up- or down-convert signals, but also allowed to provide full-duplex communication channels for both ELEMENT A and B of operation frequency near 2.4 GHz.

This designed module is included in three sub-modules: IF sub-module, local frequency sub-module and RF sub-module. The function of IF sub-module is converting the operation frequency of ELEMENT A up to 3.4 GHz, and combining itself with the signal of ELEMENT B as the IF signal. There are one voltage controlled oscillator and a phase-locked loop circuitry in the local frequency sub-module to stably give not only IF sub-module a local frequency source of 5.85 GHz, but also additional two sets of 17.55 GHz source for the transmitting and receiving RF sub-module respectively by circuitries of frequency tripler, power divider and amplifiers. The RF sub-module is applying the inner sub-harmonic mixer to converting the IF signal up to RF pass-band and then transmitting it via the antenna, or to converting the received RF signal down to IF pass band for the IF sub-module.

The final measured result: the communication distance between the on-board and road-side unit is 10 meter at the data rate of 950K bytes per second.

誌　　謝

本論文得順利完成，首先感謝鍾世忠老師於在學期間給予之指導。同時感謝在學期間幫助我的教授、同學及公司的同事。謝謝我的父母歐聰勇先生和歐曾彩紅女士三十年來的辛苦栽培及支持，在此獻上個人最崇高的敬意與謝意。

歐宗信 民國九十五年九月 于交通大學

INDEX

ABSTRACT(CHINESE) i
ABSTRACT(ENGLISH) ii
ACKNOWLEGEMENT iii
INDEX iv
CHAPTER 1 INTRODUCTION 1
1.1 Background of this thesis 1
1.2 Chapter outline 1
CHAPTER 2 ARCHITECTURE 3
2.1 Architecture of Ka band HUB diplexer module 3
2.2 Operation 6
2.2.1 Downlink 6
2.2.2 Uplink 6
CHAPTER 3 DESIGN APPROACH 8
3.1 local frequency sub-module 8
3.1.1 Matching of Ku band amplifier 9
3.1.2 Phase-locked oscillator 16
3.1.3 Design of frequency tripler 20
3.1.4 Measurement of local frequency sub-module 23
3.2 IF sub-module 24
3.2.1 Description of functional operation 25
3.2.2 Design of compact band selection filter 26
3.2.3 Measurement of IF sub-module 30
3.3 RF sub-module 32
3.3.1 Design of sub-harmonically pumped mixer 35
3.3.2 Measurement of RF sub-module 41
3.4 Modification of line-up 43
CHAPTER 4 INTEGRATED MEASUREMENT 45
4.1 Output transmitting power 45
4.2 Receiving power of down-conversion 48
4.3 Noise figure 51
4.4 Link test 54
CHAPTER 5 CONCLUSION 57
REFERENCE 58

CHAPETER 1 INTRODUCTION

1.1 Background of this thesis

To fulfill the future wireless communication needs for DSRC (Dedicated Short Range Communications) based road-to-vehicle communication (RVC), radio-on-fiber (ROF) RVC [1] and the inter-vehicle communication (IVC) in the intelligent transport system (ITS), multiple services and the high carrier-frequency with the high data transmission rate technology should be explored for the mobile broadband access.

Most of functions of RCV and IVC could be accomplished by using DSRC infrastructure. However, the existing DSRC at the microwave frequency close to 5.8 GHz with the data rate less than one mega bits per second is not sufficient to afford requirements of the large scale data bulk download in future ITS, such as Automated Highway System (AHS) and Advanced Vehicle Control and Safety System (AVCSS).

The space transmission portion of being applied to the millimeter-wave (MMW) technology, which transmits a large capacity of information within a narrow area and with the data rate more than several ten mega bits per second per advantages mentioned in [2], is a prospective candidate for future RCV and IVC.

The target of this paper is to design and fabricate one ON-BOARD UNIT (OBU), as well as ROAD-SIDE UNIT (RSU), for the application of IEEE 802.11 b or g wireless communication protocol in purpose of the convenience for the evaluation. The designed module is like

- not only HUB of providing the uplink and downlink wireless communication channel for both connected ELEMENT A and B,

- but also a diplexer allowing dual WLAN module pairs to transmit and receive data, respectively and independently.

In this paper, OBU (or RSU) of functions described and operated above is so named Ka band HUB diplexer module.

1.2 Chapter outline

This paper consists of five chapters.

Chapter 1 introduces the background of this thesis.

Chapter 2 describes the architecture and operation of Ka band HUB diplexer module.

Chapter 3 describes the design approach and the development of each sub-module.

Chapter 4 presents how to measure the performance of Ka band HUB diplexer module and results of the measurement.

Chapter 5 is the conclusion of this paper.

CHAPETER 2 ARCHITECTURE

2.1 Architecture of Ka band HUB diplexer module

Figure 2-1 shows the structure diagram of RVC system included in OBU fixed into the traveling vehicle and RSU located on the top of tower near the roadside base station (or the control center).

Both of them provide two connected ports as marked as ELEMENT A and B (linked to IEEE 802.11 b or g module, in this paper), respectively.

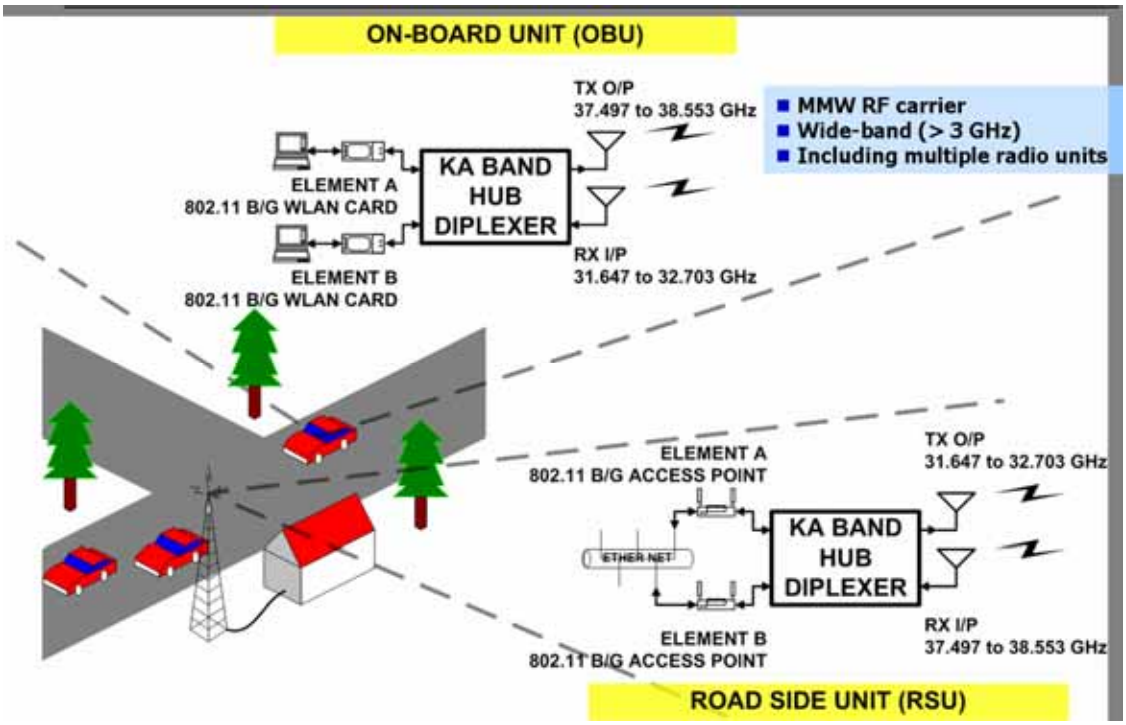

Figure 2-1 – the structure diagram of RCV system

The wireless communication of uplink path (form OBU to RSU) uses the MMW frequency band from 37.497 to 38.553 GHz, and of downlink path (from RSU to OBU) is from 31.647 to 32.703 GHz.

The total transmission band width is 2.112 GHz among the overall carrier frequency band width of 6.906 GHz.

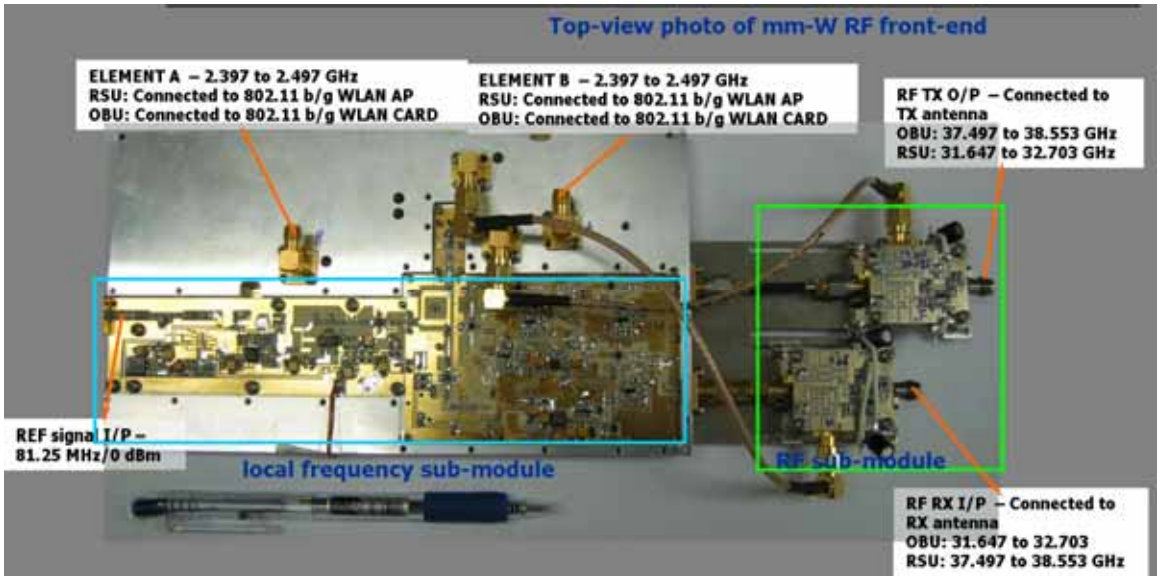

Graph 2-1 – the top-side view photograph of RSU (or OBU)

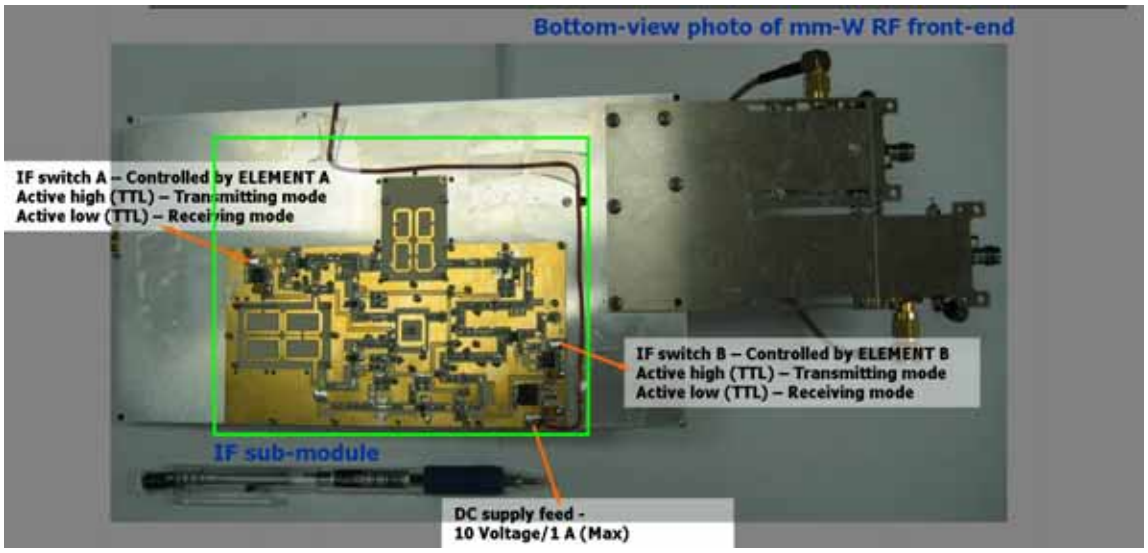

Graph 2-2 – the bottom-side view photograph of RSU (or OBU)

As the block diagram shown in Figure 2-2 and photographs of Graph 2-1 and 2-2, there are three sub-modules in a Ka band HUB diplexer module: IF, local frequency and RF sub-module.

The whole circuitries of both IF and local frequency sub-module are assembled on the commercial soft board, RO4003, with the 20 mil thickness and the half once conducting copper.

To reduce the path loss and the fabrication tolerance in the dimension of circuitries designed at the Ka frequency band, the RF sub-module is fabricated on the high dielectric material, such as Al2O3 with the 10 mil thickness and the dielectric constant of 9.8, by the standardized and well-controlled thin-film process.

With the frequency division duplex (FDD) technology applied in the RF-sub module and the usage of the time division duplex (TDD) scheme in the IF sub-module, the connection between ELEMENT A of OBU and of RSU is independent of the link between ELEMNT B of OBU and of RSU.

In a word, the kernel design concepts in this paper are developing a sub-module, like the IF sub-module, of the multiplexing function to let several communication services share the RF carrier frequency band width and propagate in air by the MMW technology in the RF sub-module.

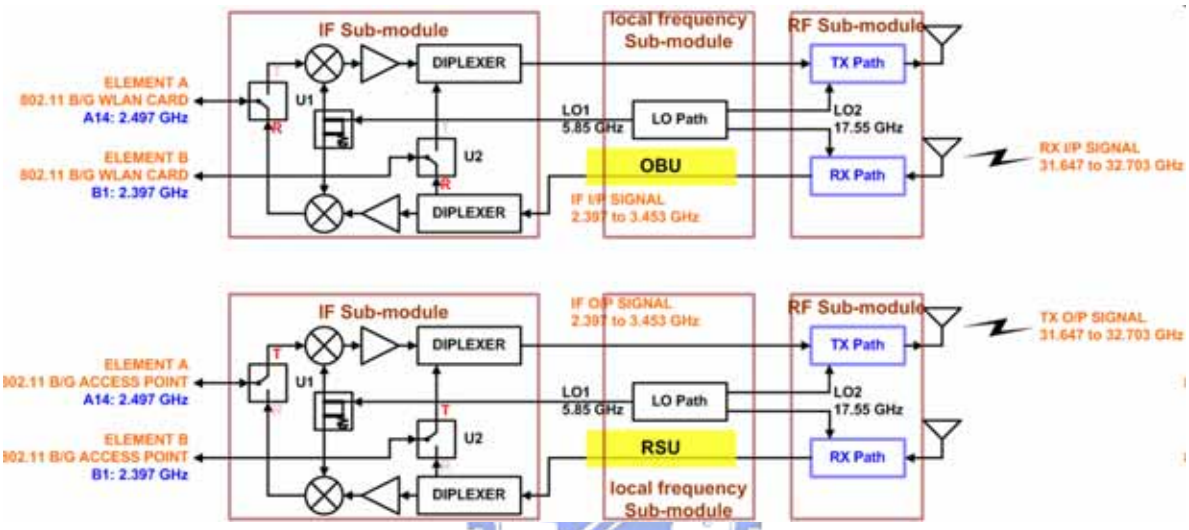

Figure 2-2 – the block diagram of the RX downlink path (from RSU to OBU)

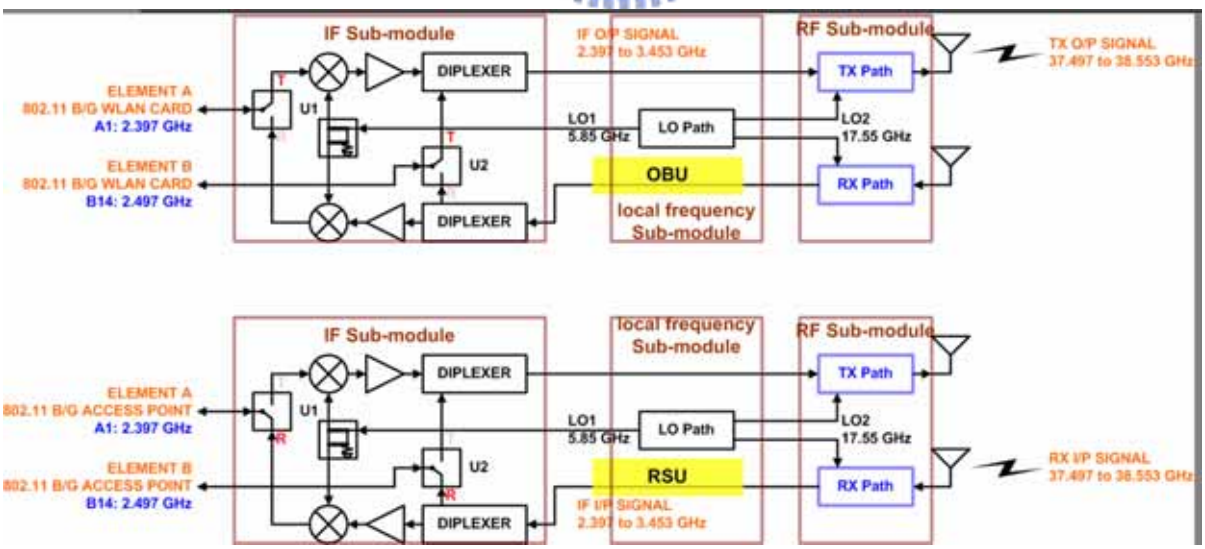

Figure 2-3 – the block diagram of the TX uplink path (from OBU to RSU)

Inside circuitries of OBU are same as RSU each other, except the output transmitting power. The reason that the transmitting carrier-frequency band of RSU is chosen close to 32 GHz is due to

the MMIC (Monolithic Microwave Integrated Circuit) amplifier in the RF sub-module having the better performance of the output power at 32 GHz than at 38 GHz.

2.2 Operation

2.2.1 Downlink

According to Figure 2-2 shown above, for examples, assume that the signal of ELEMENT B is acknowledged to be B1 of the frequency at 2.397 GHz and the signal of ELEMENT A is A14 of the frequency at 2.497 GHz.

The downlink path is form the transmitting of RSU to the receiving of OBU. The procedure of downlink operation could be broken-down into several steps and described as below.

Step 1: In the IF sub-module of RSU, A14 is up-converted to 3.353 GHz by the inner mixer and the local source of 5.85 GHz, marked as LO1, from the local frequency sub-module.

Step 2: It combines the up-converted A14 with B1 as output IF signals by making the use of the diplexer in the IF sub-module of RSU.

Step 3: Having been mixed with LO2 (17.55 GHz) via the sub-harmonically pumping mixer (SHPM) of the TX path in the RF sub-module of RSU, A14 and B1 are converted up to 31.747 and 32.703 GHz, severally, and then amplified into the downlink receiver, such as OBU, by going through the MMIC amplifier and the outside TX antenna.

Step 4: Weakly RF signals received by OBU are amplified by the MMIC LNA (Low Noise Amplifier) of the RX path in the RF sub-module, and then converted down to IF frequencies by the SHPM in the same path.

Step 5: In the IF sub-module of OBU, A14 and B1 are separated by the inner diplexer circuitry. With the inside discrete mixer, A14 at 3.353 GHz is down-conversed to the frequency at 2.497 GHz and received by the connected WLAN module.

2.2.2 Uplink

The uplink path of Figure 2-3 is defined from the transmitting of OBU to receiving of RSU. For examples, there is a WLAN modulated signal of ELEMENT A as referred to A1 of the frequency at 2.397 GHz and so is B14 of the frequency at 2.497 GHz regarding to ELEMENT B.

The procedure of uplink operation could be broken-down several steps and described as below.

Step 1: In the IF sub-module of OBU, A1 is converted up to 3.453 GHz by the mixing with LO1 (5.85 GHz).

Step 2: It combines the up-converted signal of A1 with B14 as the output IF signal by the diplexing component in the IF sub-module of OBU.

Step 3: Having been mixed with LO2 (17.55 GHz) via the SHPM of the TX path in the RF sub-module of OBU, A14 and B1 are converted up to 38.553 and 37.597 GHz, respectively, and then amplified into the uplink receiver, such as RSU, by going through the MMIC amplifier and the outside TX antenna.

Step 4: Weakly RF signals received by RSU are amplified by the MMIC LNA in the RF RX sub-module, and then converted down to IF frequencies by the inside SHPM.

Step 5: In the IF sub-module of RSU, A1 and B14 are separated by the inner diplexer. With the inside mixer, A1 at 3.453 GHz is down-conversed to the signal at 2.397 GHz and received by the connected WLAN module.

Briefly, the different usage bands of uplink and downlink operation improves the isolation between the transmitting and receiving in the RF sub-module.

The IF sub-module is much like the multiplexer and having the frequency shift capability to contribute a frequency spacing of 856 MHz between ELEMENT A and B.

Regarding to the application for multiple servicings of high quantity elements, the design scheme of multiplexing sub-module and considerations of frequency plan will become more complex and expensive with respect to sub-circuitries in sub-modules. Furthermore, the isolation between each element will be also an uneasy solved issue.

CHAPTER 3 DESIGN APPROACH

The design flow of this paper is the approach of BOTTOM-to-UP by the tabular line-up analysis of the gain budget. To define the frequency plan and spacing between elements is the first step of design procedure in this paper.

3.1 Local frequency sub-module

The block diagram of local frequency sub-module is described in Figure 3-1. In this case, this sub-module is implemented with

- Phase-locked oscillator (PLO) of 5.85 GHz, referred to LO1, at the middle-top portion of Graph 3-1 converses signals of ELEMENT A up to the frequency band from 3.353 to 3.453 GHz and makes the frequency spacing of 856 MHz between ELEMENT A and B.

- The signal flowing path works one local source pair of LO2 (17.55 GHz) needed for the sub-harmonically pumping mixer (SHPM) of RF sub-module at the right side of Graph 3-1.

With the adjustable reference signal of 81.25 MHz at the left side of Graph 3-1, this loop circuitry will be locked at 5.85 GHz to vanquish the synchronization issue between OBU and RSU.

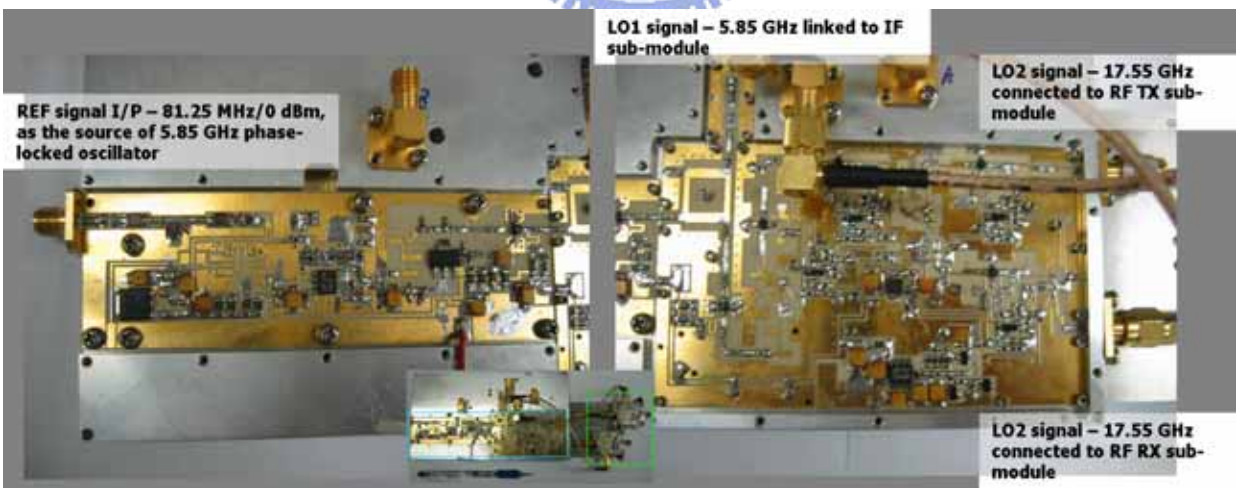

Graph 3-1 the top photograph view of local frequency sub-module

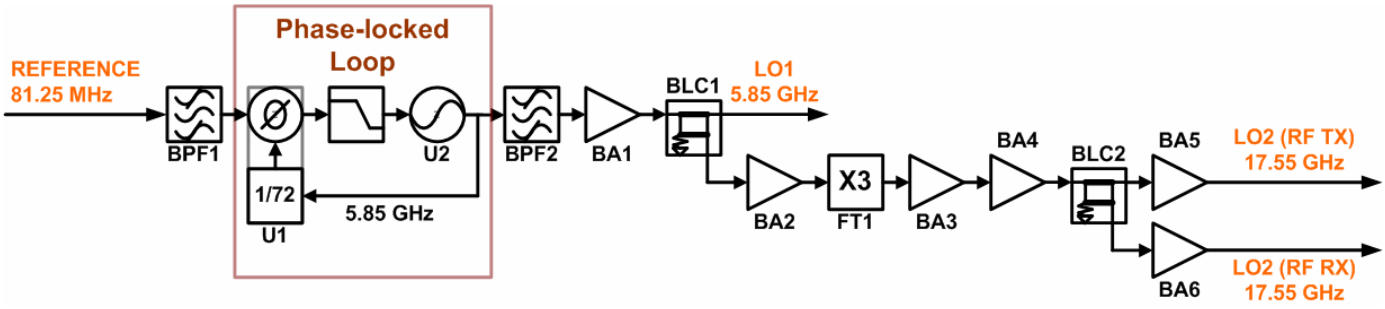

Figure 3-1 the block diagram of local frequency sub-module

In details, there are existing three output local sources in the local frequency sub-module

- LO1, connected to the IF sub-module, does be obtained by the locked signal of 5.85 GHz going through the filtering of BPF2, the amplifying of BA1 (ERA-1SM manufactured by MINI-CIRCUITS) and the equal power splitting of BLC1 in series.

- LO2 (17.55 GHz), connected to the RF TX sub-module, does be the triple frequency signal of LO1 by going through the signal flowing path consisted of the amplifying gain block which contains ERA-1SM of BA2, 3 and 4 and NE3210S01 of BA5, the frequency multiplying of FT1 and the equal power dividing of BCL2.

- LO2 (17.55 GHz), connected to the RF RX sub-module, is another output of BCL2, which is amplified by BA6 (NE3210S01).

The gain budget table of local frequency sub-module is figured out as Table 3-1, based on the gain or loss from the data sheet of discrete components and simulated results. Per the line-up analysis, the assumed output power of LO1 is 6 dBm and LO2 is 7 dBm.

Sub-module: Local frequency

	BPF2		BA1	BCL1	BA2	FT1	BA3	BA4	BCL2	BA5
	LPF	HPF								
Gain / Loss (dB): Design goal	-1.5	-1.5	10.0	-4.0	10.0	-25.0	9.0	9.0	-5.0	9.0
Input power (dBm) per stage	5.0	3.5	2.0	10.0	6.0	10.0	-15.0	-6.0	3.0	-2.0
Output power (dBm) per stage proposed 5 dBm output power of PLO (U2)	3.5	2.0	10.0	6.0	10.0	-15.0	-6.0	3.0	-2.0	7.0
				LO1						LO2

Table 3-1 the gain budget table of local frequency sub-module

3.1.1 Matching of Ku band amplifier

Due to LO2 being a single tone source at 17.55 GHz, the driven amplifier design for LO2 is realized by following the simultaneous conjugate matching introduced in [3] for the maximum transducer gain.

Step 1 - Stability

Before designing the Ku band amplifier, it is important and the first step to check the stability of device and take considerations with the choke circuitry of the DC supply feed at the same time.

Choke circuitry:

The geometry and simulation results of the choke circuitry are presented in Figure 3.1.1-1.

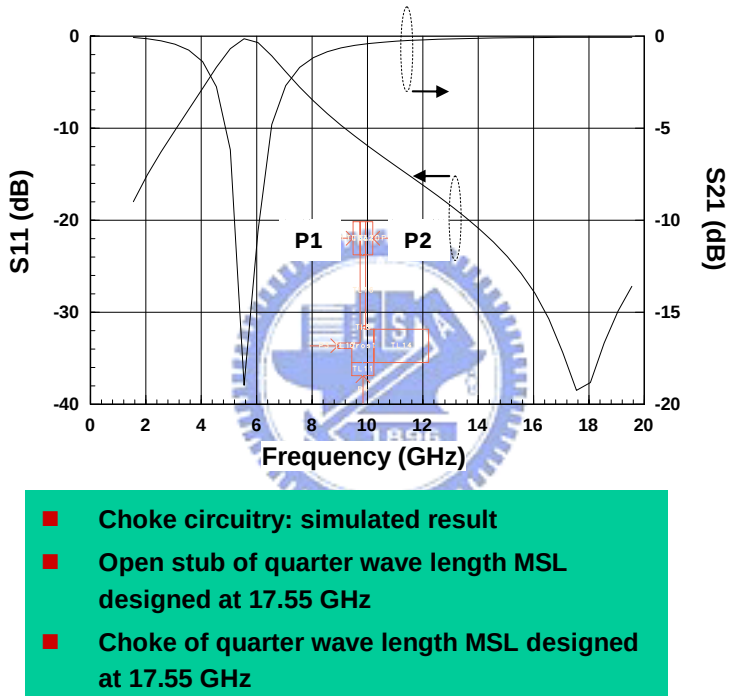

Figure 3.1.1-1 the geometry and simulation results of the choke circuitry

Calculation of stability:

With following equations of input and output stability circle, it is simple to check the stability of NE3210S01.

$$\Delta = S_{11}S_{22} - S_{12}S_{21}$$ - Equation (3.1.1.1)

$$K = \frac{1-|S_{11}|^2-|S_{22}|^2+|\Delta|^2}{2|S_{12}S_{21}|}$$ - Equation (3.1.1.2)

The following equation is the radius of the input stability circle given by

$$r_S = \left| \frac{S_{12}S_{21}}{|S_{11}|^2 - |\Delta|^2} \right| \quad \text{- Equation (3.1.1.3)}$$

And the center of the input stability circle is obtained from

$$C_S = \frac{\left(S_{11} - \Delta S_{22}^*\right)^*}{|S_{11}|^2 - |\Delta|^2} \quad \text{- Equation (3.1.1.4)}$$

Regarding to the radius of the output stability circle, it is given by

$$r_L = \left| \frac{S_{12}S_{21}}{|S_{22}|^2 - |\Delta|^2} \right| \quad \text{- Equation (3.1.1.5)}$$

And the center of the output stability circle could be given by the following equation

$$C_L = \frac{\left(S_{22} - \Delta S_{11}^*\right)^*}{|S_{22}|^2 - |\Delta|^2} \quad \text{- Equation (3.1.1.6)}$$

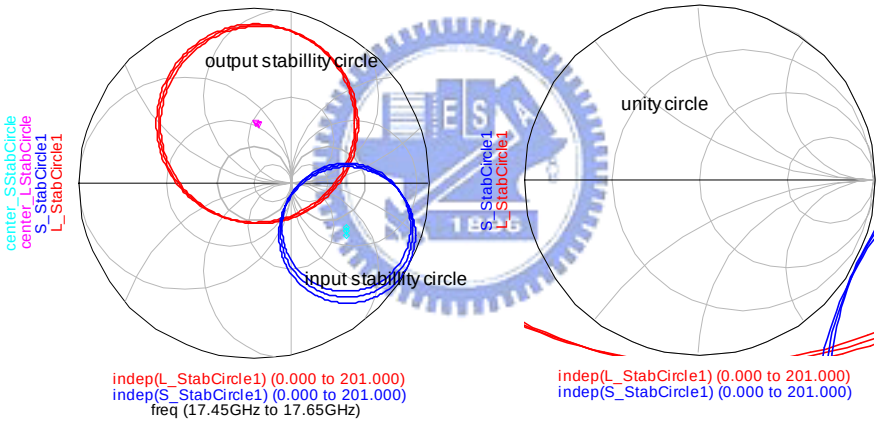

freq	center_LStabCircle	radius_LStabCircle	center_SStabCircle	radius_SStabCircle
17.45 GHz	1.569 / 84.599	2.642	2.852 / -29.053	1.823
17.55 GHz	1.587 / 86.543	2.650	2.796 / -27.289	1.771
17.65 GHz	1.605 / 88.470	2.656	2.741 / -25.514	1.721

freq	delta	K
17.45 GHz	0.513 / 17.158	1.045
17.55 GHz	0.517 / 13.996	1.038
17.65 GHz	0.521 / 10.824	1.032

freq	S(1,1)	S(1,2)	S(2,1)	S(2,2)
17.45 GHz	0.665 / 17.888	0.115 / -81.496	2.843 / -104.457	0.374 / 30.274
17.55 GHz	0.671 / 16.028	0.115 / -83.026	2.819 / -106.555	0.381 / 28.441
17.65 GHz	0.677 / 14.158	0.115 / -84.562	2.796 / -108.660	0.388 / 26.592

Figure 3.1.1-2 K and Δ calculated table with port stability circles

In the table shown in Figure 3.1.1-2, the two-port network is unconditionally stable

with $K>1$ and $|\Delta|<1$ from 17.4 to 17.7 GHz.

According to stability circles, if it terminates the output port (as well as the input port) of NE3210S01 with the loading impedance of 50 OHM. The load reflection coefficient of Γ_L (as well as the source refection coefficient of Γ_S) looking into the input port of load (as well as the output port of source) shell be zero, that would lead to the input reflection coefficient equaling to S_{11} (as well as S_{22} with respect to the output refection coefficient) and having the magnitude value less then one.

Per the Γ_L plane (as well as the Γ_S plane) plotted on the smith chart, the chosen point of Γ_L (as well as Γ_S) at the center of the unity circle will let the magnitude of output reflection coefficient (as well as the input reflection coefficient) be less than one. It is meaning the region enclosed by the output stability and unity circle is stable (as well as the region of inner unity circle to the input stability circle).

Step 2 - Input matching network

The source reflection coefficient looking into the output port of the input matching network is obtained by

$$\Gamma_{MS}=\frac{B_1-\sqrt{B_1^2-4|C_1|^2}}{2C_1}$$ - Equation (3.1.1.7)

Where,

$$B_1=1+|S_{11}|^2-|S_{22}|^2-|\Delta|^2$$

$$C_1=S_{11}-\Delta S_{22}^*$$

The input reflection coefficient looking into the input port of the FET is

$$\Gamma_{IN}=\Gamma_{MS}^*$$

The source impedance looking into the output port of the input matching network is given by

$$Z_S=Z_0\frac{1+\Gamma_{MS}}{1-\Gamma_{MS}}$$ - Equation (3.1.1.8)

Per equation (3.1.1.7), (3.1.1.8), (3.1.1.9) and (3.1.1.10), the calculated design goal of source and load impedance at the frequency point of 17.55 GHz is shown in Figure 3.1.1-3.

freq	gamma_IN	gamma_MS
17.45 GHz 17.55 GHz 17.65 GHz	0.825 / 29.053 0.839 / 27.289 0.854 / 25.514	0.722 - j0.401 0.745 - j0.385 0.770 - j0.368

freq	gamma_OUT	gamma_ML
17.45 GHz 17.55 GHz 17.65 GHz	0.613 / 95.401 0.638 / 93.457 0.665 / 91.530	-0.058 - j0.611 -0.038 - j0.636 -0.018 - j0.665

freq	Z_S	Z_L
17.45 GHz 17.55 GHz 17.65 GHz	66.866 - j168.296 69.675 - j180.812 72.178 - j195.671	20.901 - j40.940 20.005 - j42.902 18.850 - j44.994

- **Z_S, source impedance: looking into the output port of the source**
- **Z_L, load impedance: looking into the input port of the load**
- **gamma_MS, source reflection coefficient: looking into the output port of the input matching network**
- **gamma_ML, load reflection coefficient: looking into the input port of the output matching network**

Figure 3.1.1-3 the calculated design goal of source and load impedance at 17.55 GHz

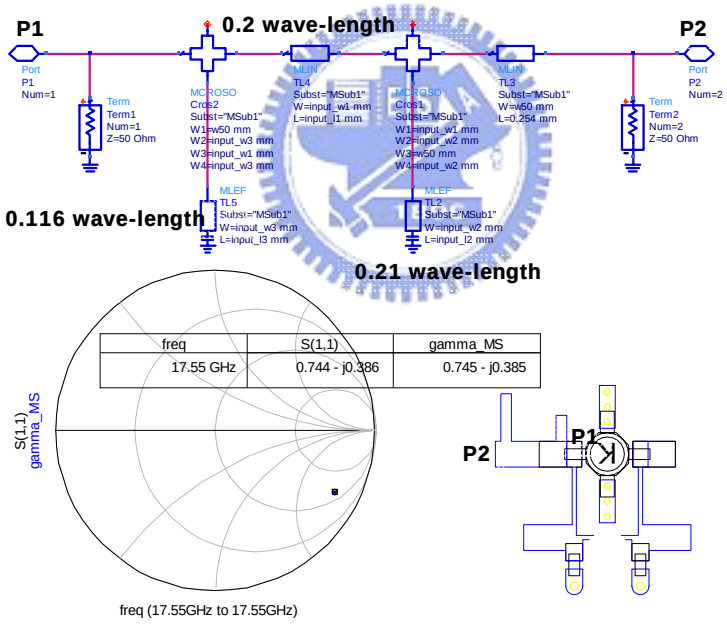

- **Schematic drawing of input network and simulation result**
- **P1 : looking into the output port of input matching network**
- **P2 : as connected to the source port with fifty OHM load**

Figure 3.1.1-4 the schematic drawing of matched input network and the simulation result

As shown in Figure 3.1.1-4, due to P2 connected to the 50 OHM source, the reflection coefficient looking into P1 equals to S11 of the input matching network. With the shunted open-stub of 0.21 wave-length, the serried MSL of 0.2 wave-length and the shunted open-stub of 0.116

wave-length nearby P1, S11 is almost same as the refection coefficient of Γ_{MS} .

Step 3 - Output matching network

The load reflection coefficient looking into the input port of the output matching network is

$$\Gamma_{ML} = \frac{B_2 - \sqrt{B_2^2 - 4|C_2|^2}}{2C_2} \quad \text{- Equation (3.1.1.9)}$$

Where,

$$B_2 = 1 + |S_{22}|^2 - |S_{11}|^2 - |\Delta|^2$$

$$C_2 = S_{22} - \Delta S_{11}^*$$

The output reflection coefficient looking into the output port of the FET is

$$\Gamma_{OUT} = \Gamma_{ML}^*$$

The load impedance looking into the input port of the output matching circuit is

$$Z_L = Z_0 \frac{1+\Gamma_{ML}}{1-\Gamma_{ML}} \quad \text{- Equation (3.1.1.10)}$$

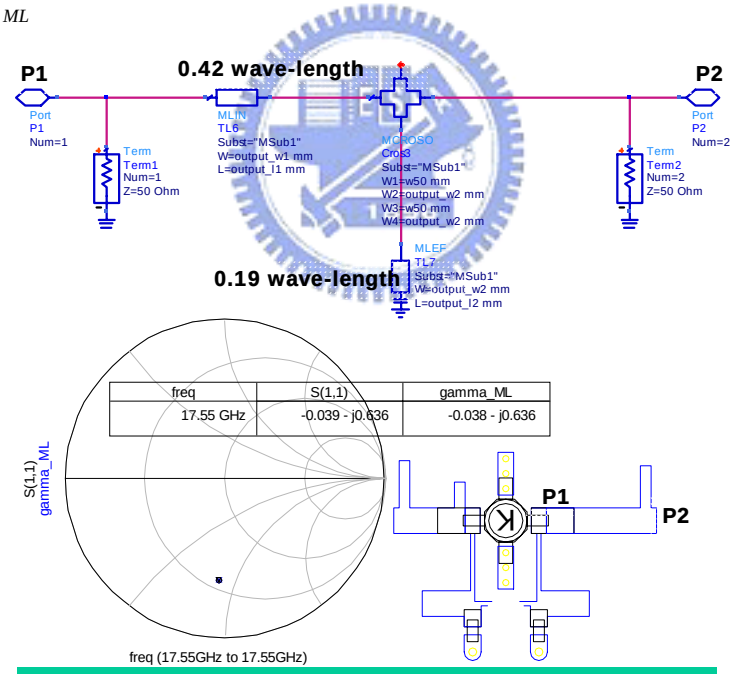

- **Schematic drawing of output network and the simulation result**
- **P1 : looking into the input port of output matching network**
- **P2 : as connected to the load port with fifty OHM load**

Figure 3.1.1-5 the schematic drawing of matched output network and the simulation result

As shown in Figure 3.1.1-5, due to P2 connected to the 50 OHM load, the reflection coefficient looking into P1 is S11 of the network. With the shunted open-stub of 0.19 wave-length and the

serried MSL of 0.42 wave-length connected to P1, S11 is almost same as the refection coefficient of Γ_{ML} .

Step 4 - DC block circuit

In order to saving the propagation loss due to the degraded electrical performance of lumped capacitor during the high frequency band, the small gap edge coupler line with the design of 10% band width at 17.55 GHz is planned instead of the lumped capacitor. Figure 3.1.1-6 is the simulation result within attaching the geometry layout of the DC blocking circuitry.

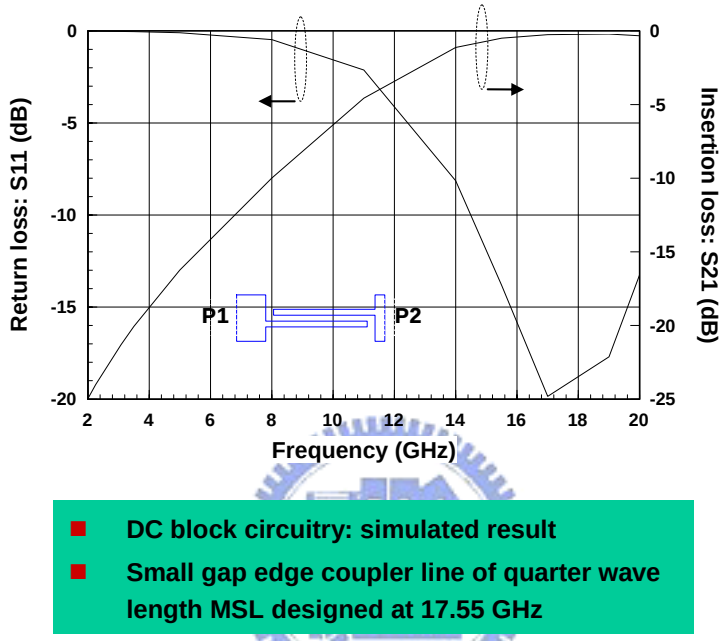

Figure 3.1.1-6 the simulation result of DC block circuit and geometry

Step 5 – Integrated simulation performance

Having combined NE3210S01 with well-matched input and output networks and the blocking circuitry, the integrated simulation result of whole sub-block is shown in Figure 3.1.1-7. It presents that

- The port return loss at 17.55 GHz is less than -20 dB
- The transducer gain from 14.45 to 14.65 GHz is greater than 11 dB with the point-to-point gain flatness less than 0.5 dB.

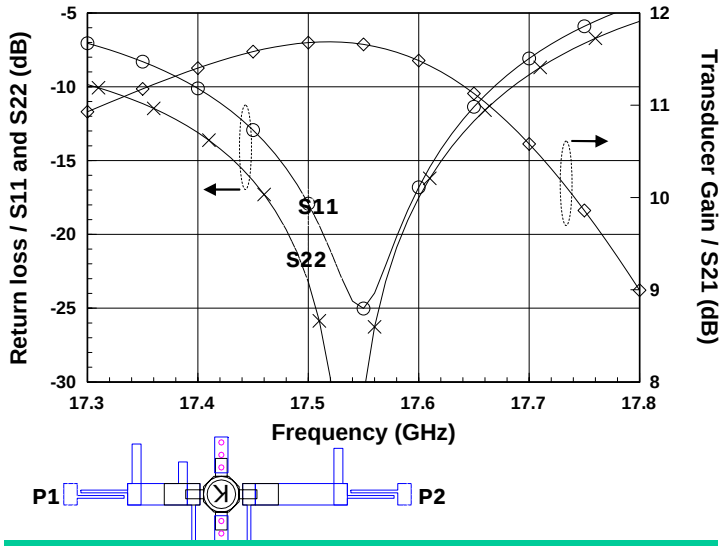

Figure 3.1.1-7 the integrated simulated result of local frequency amplifier

3.1.2 Phase-locked oscillator (PLO)

The schematic drawing of PLO is shown in Figure 3.1.2-1 from the application note of U1.

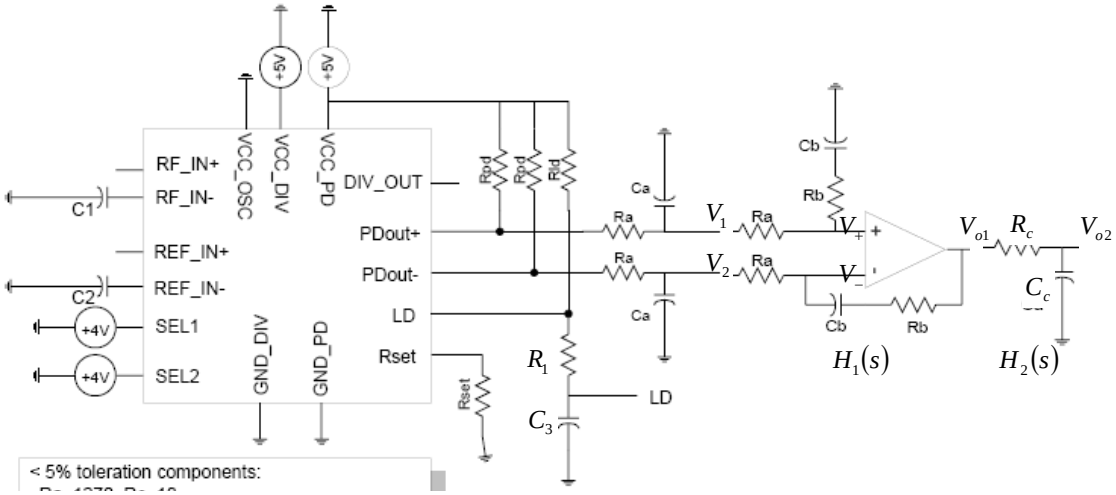

Figure 3.1.2-1 the schematic configuration of connections between U1, U2 and the loop filter in the phased-locked loop circuitry

From the recommended schematic configuration, the loop filter between U1 and U2 is applied the signal flow of differential-input and single–output scheme to make the use of operation amplifier.

The filter is consisted of

- The order two active filter which is consisted of R_a, R_b, C_a and C_b

- The order one passive filter which is serried with a resistor, R_c, and shunted with a lumped capacitor, C_c, for the suppression of close-in spurious greater than 10 MHz.

The transferring function of this order two filter of $H_1(s)$ is solved from

EQUATION (i): $V_+ = V_1 \dfrac{R_b + \dfrac{1}{sC_b}}{R_a + R_b + \dfrac{1}{sC_b}}$ by the infinite input impedance of the ideal operation amplifier and the rule of KVL

EQUATION (ii): $V_+ = V_-$ based on the ideal characteristic of operation amplifier

EQUATION (iii): $\dfrac{V_2 - V_-}{R_a} = \dfrac{V_- - V_{o1}}{R_b + \dfrac{1}{sC_b}}$ by the rule of KCL

EQUATION (iv): $\dfrac{PD_{out+} - V_1}{R_a} + \dfrac{-V_1}{\dfrac{1}{sC_a}} = \dfrac{V_1 - V_+}{R_a}$ and $\dfrac{PD_{out-} - V_2}{R_a} + \dfrac{-V_2}{\dfrac{1}{sC_a}} = \dfrac{V_2 - V_-}{R_a}$ by the rule of KCL.

From EQUATION (ii) and (iv), it gives

$V_1 - V_2 = \dfrac{PD_{out+} - PD_{out-}}{2 + sR_aC_a}$ - Equation (3.1.2.1)

From EQUATION (i), (ii) and (iii), the relationship between V_1, V_2 and V_{out1} is

$V_1 - V_2 = V_{out1} \dfrac{R_a}{R_b + \dfrac{1}{sC_b}}$ - Equation (3.1.2.2)

Submitting equation (3.1.2.2) into equation (3.1.2.1), $H_1(s)$ can be obtained by

$$H_1(s) = \frac{V_{out1}}{PD_{out+} - PD_{out-}} = \frac{1 + sR_bC_b}{(sR_aC_b)(2 + sR_aC_a)}$$ - Equation (3.1.2.3)

The transfer function of the passive filter of $H_2(s)$ is given by following up the rule of KVL

$$H_2(s) = \frac{V_{out2}}{V_{out1}} = \frac{1}{1 + sR_cC_c}$$ - Equation (3.1.2.4)

Thus, the fully transfer function of $H(s)$ is yielded from equation (3.1.2.3) and (3.1.2.4)

$$H(s) = H_1(S) * H_2(s) = \frac{1 + sR_bC_b}{(sR_aC_b)(2 + sR_aC_a)(1 + sR_cC_c)}$$ - Equation (3.1.2.5)

Close-loop:

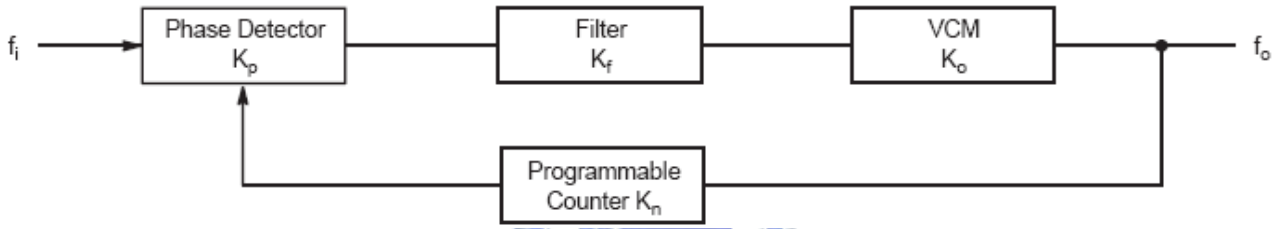

Figure 3.1.2-2 the close –loop diagram of PLO

Figure 3.1.2-2 is the close-loop diagram of the PLO to be broken-down into several portions

- K_p is the differential gain constant of the phase detector and, in this case, it is written by

$K_p = \frac{2 * 1.65V}{2\prod} = 0.526$ Voltage/Radian, when the reference input frequency is equal to 100 MHz

- K_f does be the transfer function of $H(s)$ within lumped components in the schematic configuration being

$Ra = 2000OHM$; $Ca = 68\,pF$; $Rb = 4700OHM$; $Cb = 1000\,pF$; $Rc = 39.2OHM$; $Cc = 100\,pF$

- K_v is defined as the sensitivity of VCO in radians per second per voltage. From the device data sheet of U2, it is found by

$$K_v = 2\prod * \left(150\frac{MHz}{Voltage}\right) = 0.942E + 009 \quad \text{Radian/Second/Voltage}$$

Thus, the transfer function of VCO is given by

$$K_o = \frac{K_v}{s} \quad \text{Radian/Second/Voltage}$$

. The s in the denominator converts the frequency characteristics of the VCO to phase, i.e., the phase is the integral of frequency.

- K_n is the feedback transfer function of the $1/72$ frequency divider and integrated in U1. It is the constant gain and is presented by

$$K_n = \frac{1}{72}$$

The transfer function, as well as the close-loop gain, of the close-loop scheme as shown in Figure 3.1.2-2 is obtained by

$$H_{close-loop}(s) = \frac{K_p K_f K_o}{1 + K_p K_f K_o K_n} \quad \text{- Equation (3.1.2.6)}$$

Open-loop:

The transfer function, as well as the open-loop gain, is obtained by

$$H_{open-loop}(s) = K_p K_f K_o \quad \text{- Equation (3.1.2.7)}$$

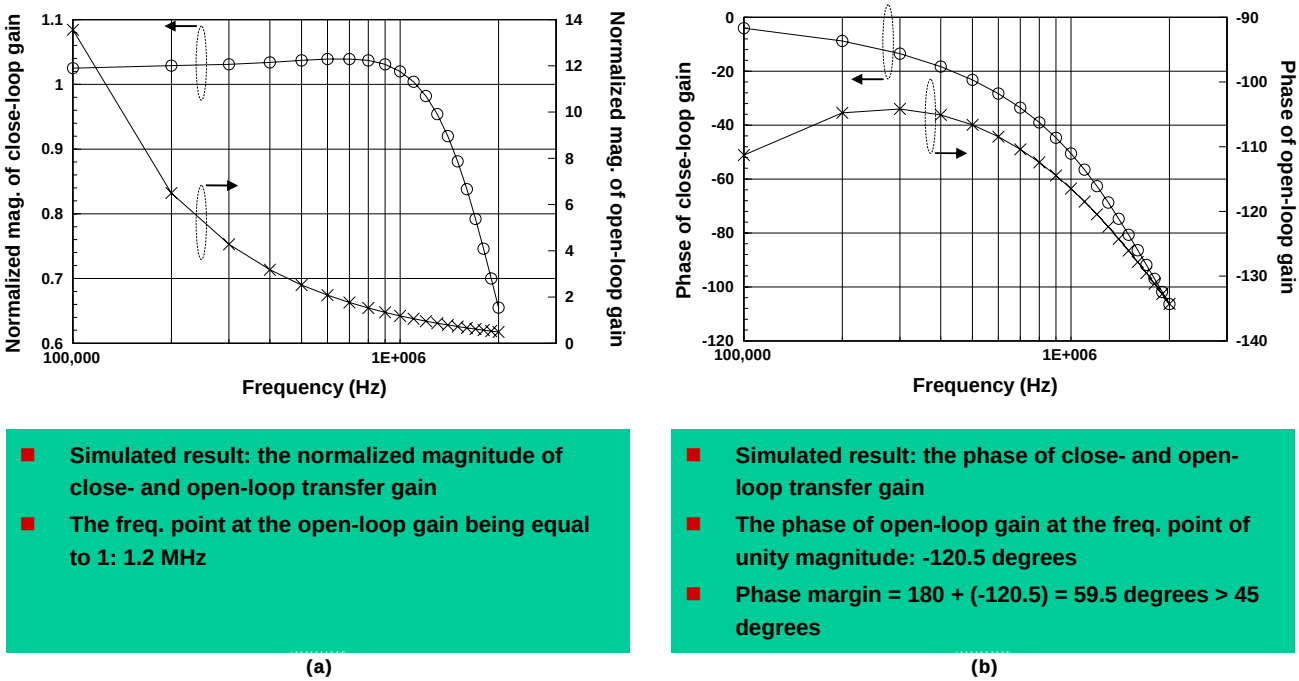

Figure 3.1.2-3 the simulation results of (a) normalized magnitude (b) phase margin of open- and close-loop transfer function

Figure 3.1.2-3 (a) is the simulated result of the normalized magnitude of open- and close-loop gain. The frequency point at the open-loop gain being one is 1.2 MHz.

Figure 3.1.2-3 (b) is showing the simulated result of the phase of open- and close-loop transferring function. At the frequency point of 1.2 MHz, the phase of the open-loop gain is -120.5 degrees leading to the phase margin of 59.5 degrees which is greater than 45 degrees to make the close-loop stable in the PLO sub-block.

3.1.3 Design of frequency-tripler

Based on the mathematical equations described in [4], the given Figure 3.1.3-1 is the circuit of anti-parallel Schottky diode pair. The currents through the diodes i_1 and i_2 are written in the usual form

$$i_1 = -i_0\left(e^{-\alpha V} - 1\right) \text{ - Equation (3.1.3.1)}$$

$$i_2 = -i_0\left(e^{\alpha V} - 1\right) \text{ - Equation (3.1.3.2)}$$

, where α is the diode slope parameter ($\alpha \approx 38V^{-1}$ for typical high-quality gallium arsenide

Schottky barrier diodes). The differential conductance for each diode is written as

$$g_1 = \frac{di_1}{dV} = \alpha i_0 e^{-\alpha V}$$ - Equation (3.1.3.3)

$$g_2 = \frac{di_2}{dV} = \alpha i_0 e^{\alpha V}$$ - Equation (3.1.3.4)

The summarization of individual conductance is given by

$$g = g_1 + g_2 = \alpha i_0 e^{-\alpha V} + \alpha i_0 e^{\alpha V} = \alpha i_0 \left(e^{-\alpha V} + e^{\alpha V}\right) = 2\alpha i_0 \cosh(\alpha V)$$ - Equation (3.1.3.5)

For the general case in which LO1 modulates the conductance of the diodes may be substituted

$$V = V_{LO1} \cos(\omega_{LO1} t)$$ - Equation (3.1.3.6)

into equation (3.1.3.5) with the following result

$$g = 2\alpha i_0 \cosh(\alpha V_{LO1} \cos(\omega_{LO1} t))$$ - Equation (3.1.3.7)

, which is expanded in the following series

$$g = 2\alpha i_0 \left[I_0(\alpha V_{LO1}) + 2I_2(\alpha V_{LO1})\cos(2\omega_{LO1} t) + 4I_4(\alpha V_{LO1})\cos(4\omega_{LO1} t) + ...\right]$$ - Equation (3.1.3.8)

, where $I_n(\alpha V_{LO1})$ are modified Bessel functions of the second kind.

The total current expansion is

$$\begin{aligned} i = g(\frac{1}{2}V_{LO1}\omega_{LO1} t + \frac{1}{2}V_{LO1}\omega_{LO1} t) &= A\cos(\omega_{LO1} t) + B\cos(\omega_{LO1} t) + C\cos(3\omega_{LO1} t) \\ &+ D\cos(5\omega_{LO1} t) + E\cos\left[(2\omega_{LO1} + \omega_{LO1})t\right] \\ &+ F\cos\left[(2\omega_{LO1} - \omega_{LO1})t\right] + G\cos\left[(4\omega_{LO1} + \omega_{LO1})t\right] \\ &+ H\cos\left[(4\omega_{LO1} - \omega_{LO1})t\right] + ... \end{aligned}$$ - Equation (3.1.3.9)

After rearranging coefficient terms of equation (3.1.3.9), it is given by

$$i = A' \cos(\omega_{LO1} t) + B' \cos(3\omega_{LO1} t) + C' \cos(5\omega_{LO1} t) + ...$$ - Equation (3.1.3.10)

It is seen that the total current contains frequency term $n * f_{LO1}$ where n is an odd integer.

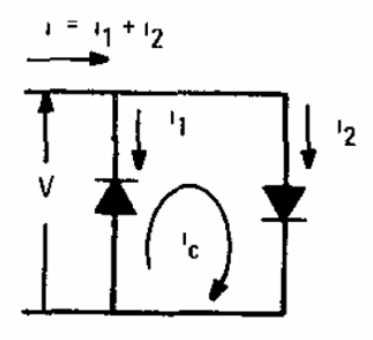

Figure 3.1.3-1 the circuit of anti-parallel diode pair

Figure 3.1.3-2 is the layout drawing with the low pass filter connected to P1 for the suppression of LO2 (17.55 GHz) and the high pass filter connected to P2 having the simulated 15 dB rejection for LO1.

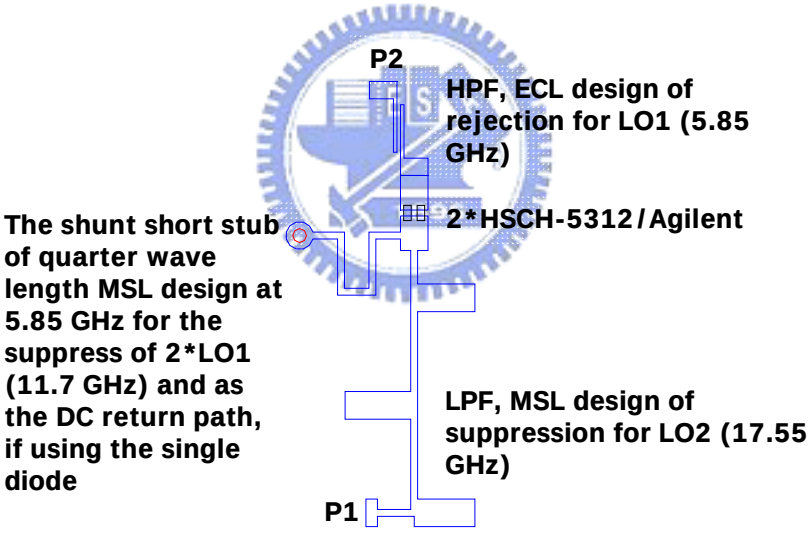

Figure 3.1.3-2 the layout drawing of frequency-tripler

Varying the injected LO1 power from 5 to 15 dBm as the X axis of Figure 3.1.3-3, simulated results of LO2 output power are plotted and referred to the left Y axis. And the right Y axis is the conversion gain of LO1 power submitting the relative LO2 power.

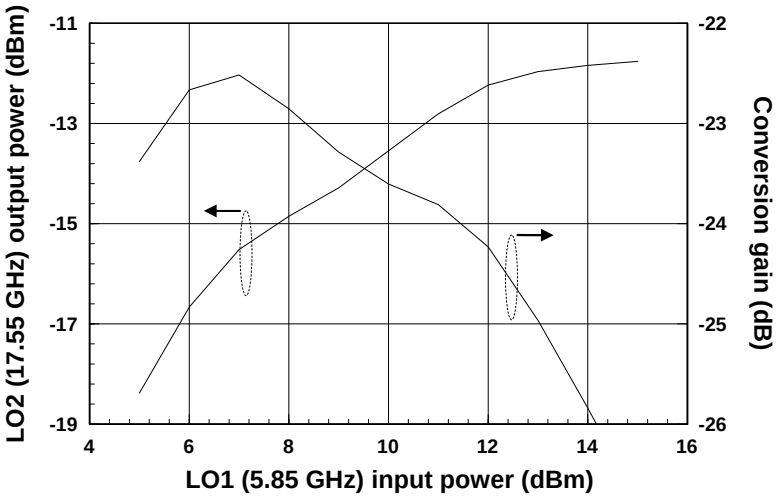

- Simulated result: LO2 of 17.55 GHz, measured at the output port of FT1 (P2)
- Conversion gain: -23.6 dB with the injected LO1 power level of 10 dBm at 5.85 GHz

Figure 3.1.3-3 the conversion gain simulated result of frequency-tripler

3.1.4 Measurement of local frequency sub-module

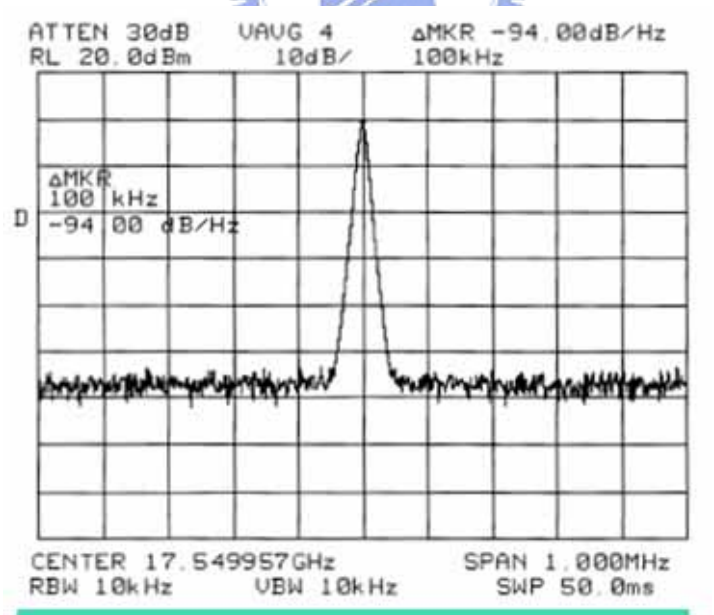

- REFERENCE input signal – injected 81.25 MHz/0 dBm by HP 8644A
- Measured at the output port of LO2
- Phase noise @ 100 KHz offset freq. away from the center freq. of 17.55 GHz: -94 dBc/Hz

Graph 3-2 the PN measured data of LO2 at 100 KHz offset frequency away form 17.55 GHz

Regarding to the phase noise (PN) measurement of LO2 as shown as Graph 3-2, the PN at 100 kHz frequency offset away from 17.55 GHz and 9 dBm output power of LO2 is -94 dBc per Hertz.

3.2 IF sub-module

With the confirmation of frequency plan and spacing between ELEMENT A and B, the next step of design procedure is for the IF sub-module. The block diagram is described in Figure 3-2.

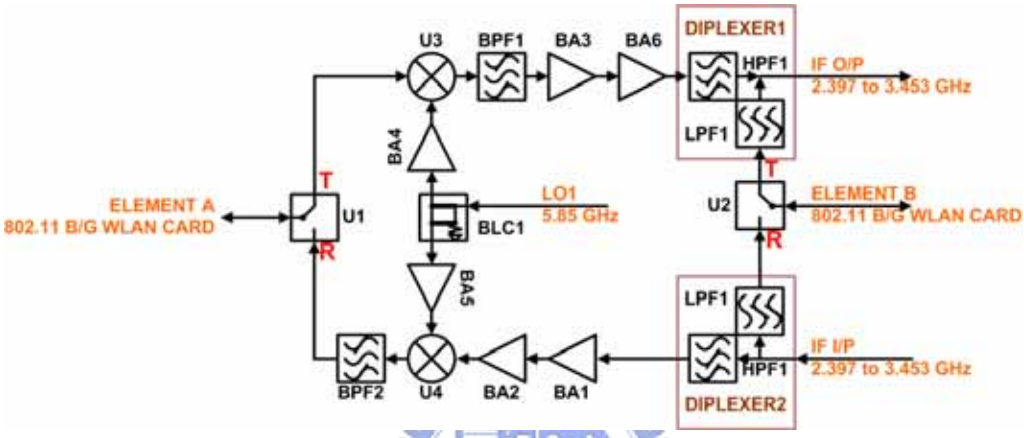

Figure 3-2 the block diagram of IF sub-module

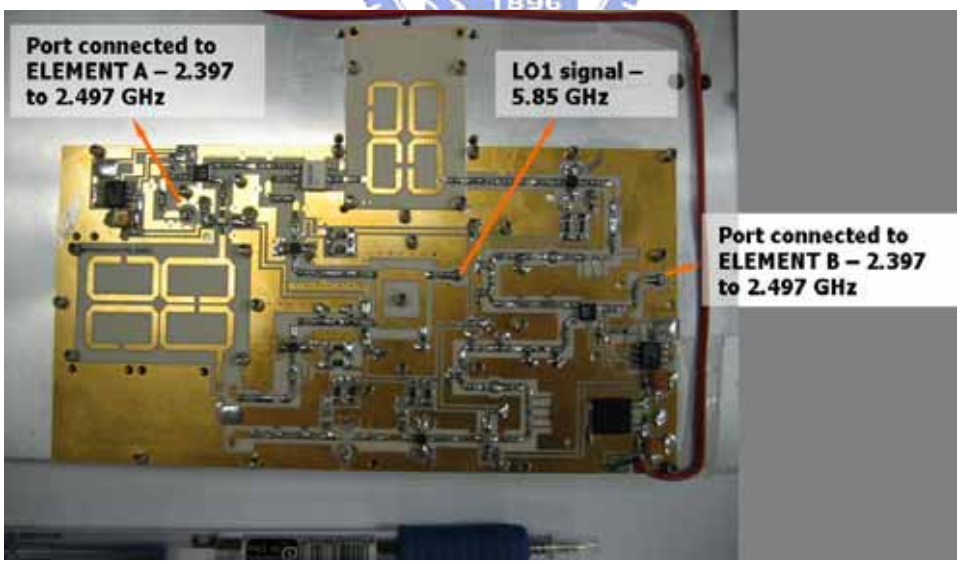

Graph 3-3 the top photograph view of IF sub-module

Per the function requirement of up- and down-conversion for ELEMENT A in the IF sub-module, there shell be existing two mixers respectively referred to U3 and U4 which is HMC168C8 manufactured by HITTITE and optional T/R (transmitting and receiving) switches

which are HMC485MS8G manufacture by HITTITE individually marked as U1 with respect to ELEMENT A and U2 to ELEMENT B.

In details,

- BA1, 2, 3 and 6 are gain amplifiers of ERA-2SM manufactured by MINI-CIRCUITS to compensate the conversion loss of ELEMENT A.

- BA4 and 5 are gain amplifiers of ERA-1SM for LO1 which is equal power splat by BLC1, and playing the role to provide the isolation between the TX and RX path of ELEMENT A.

- BPF1 and 2 are band selection filters of reduced size and different pass bands for ELEMENT A.

- Both DIPLEXER 1 and 2 have same circuitries composed of

1 The high pass filter, referred to HPF1, of the rejection band close to 2.497 GHz in the TX and RX path of ELEMENT A

2 The low pass filter, referred to LPF1, of the suppression band close to 3.353 GHz in the TX and RX path of ELEMENT B.

3.2.1 Description of functional operation

Under the TX mode of ELEMENT A (as well as ELEMENT B):

1 The T/R switch of U1 (as well as U2) is switched to the TX path, no matter ELEMENT B (as well as ELEMENT A) is under the TX or RX mode.

2 Signals of ELEMENT A mixed with LO1 via U3 are selected by BPF1 as the low side band (LSB) signals from 3.353 to 3.453 GHz and amplified by BA3.

3 Before transmitting, DIPLEXER1 combines signals of ELEMENT A through the inner HPF1 with signals of ELEMENT B through inner LPF1 as IF signals from 2.397 to 3.453 GHz.

Under the RX mode of ELEMENT A (as well as ELEMENT B):

1 The T/R switch of U1 (as well as U2) is switched to the RX path, no matter ELEMENT B (as well as ELEMENT A) is under the RX mode or not.

2 DIPLEXER2 separates IF signals down-converted form the RF RX sub-module into the frequency band from 3.353 to 3.453 GHz with the inner HPF1 for ELEMENT A and another band from 2.397 to 2.447 GHz with going through the inner LPF1 for ELEMENT B.

3 Having been amplified by BA1 and 2, signals of ELEMENT A mixed with LO1 via U4 are filtered by BPF2 as LSB signals from 2.397 to 2.497 GHz.

3.2.2 Design of compact band selection filter

The band pass filter (BPF) of four ring resonators [5] and of being lined as the U shape is taken considerations for the compact size.

Having obtained order n elements from the reference table of ladder-type low pass filter (LPF) prototype per the criteria of specifications, the filter design parameters are calculated by

$$Q_{e1} = \frac{g_0 g_1}{FBW}$$ - Equation (3.2.2.1)

$$Q_{en} = \frac{g_n g_{n+1}}{FBW}$$ - Equation (3.2.2.2)

$$M_{i,i+1} = \frac{FBW}{\sqrt{g_i g_{i+1}}}, \text{ for } i = 1 \text{ to } n+1$$ - Equation (3.2.2.3)

Among all,

- FBW is the fractional band width of the filter, which is meaning

$$FBW = \frac{\omega_2 - \omega_1}{\omega_0}$$

, where $\omega_2 - \omega_1$ is the goal of band width and ω_0 is the center frequency during the desired pass band.

- Q_{e1} and Q_{en} are the external quality factor of ring-resonators at the input and output to decide the available band width of filter by the extracting form the simulated phase and group delay response of S11 and being given by

$$Q_{e1} = \frac{f_0}{\Delta f_{\pm 90^\circ}}$$ - Equation (3.2.2.4)

, where f_0 is the frequency at the peak of group delay response and $\Delta f_{\pm 90^\circ}$ are frequencies of the 90 degrees phase difference with respect to the phase of S11 at f_0.

- $M_{i,i+1}$ are the coupling coefficients between the adjacent resonators. It can be obtained by the general formulation for the extracting

$$M_{i,i+1} = \pm \frac{f_{p2}^2 - f_{p1}^2}{f_{p2}^2 + f_{p1}^2}$$ - Equation (3.2.2.5)

, where f_{p1} and f_{p2} are frequencies at resonant points from the response of S21.

IF sub-module - BPF1:
1 the pass band from 3.353 to 3.453 GHz
2 the rejection band from 2.397 to 2.497 GHz

N=4 of ladder-type Chebyshev low pass prototype filter	g0	g1	g2	g3	g4	g5
	1	0.713	1.200	1.321	0.648	1
Center frequency (GHz)	3.473					
BW (GHz)	0.2					
FBW	7.95%					
Qei = Qeo	12.3740					
M12	0.0623					
M23	0.0457					
M34	0.0623					

(a)

IF sub-module - BPF2:
1 the pass band from 2.397 to 2.497 GHz
2 the rejection band from 3.353 to 3.453 GHz

N=4 of ladder-type Chebyshev low pass prototype filter	g0	g1	g2	g3	g4	g5
	1	0.713	1.200	1.321	0.648	1
Center frequency (GHz)	2.517					
BW (GHz)	0.2					
FBW	5.76%					
Qei = Qeo	8.9645					
M12	0.0860					
M23	0.0631					
M34	0.0860					

(b)

Table 3.2.2-1 the calculated design parameters of (a) BPF1 (b) BPF2 in the IF sub-module

Submitting parameters of Chebyshev LPF prototype into the equation (3.2.2.1), (3.2.2.2) and (3.2.2.3), Table 3.2.2-1 (a) is calculated results of BPF1 and so is Table 3.2.2-1 (b) for BPF2.

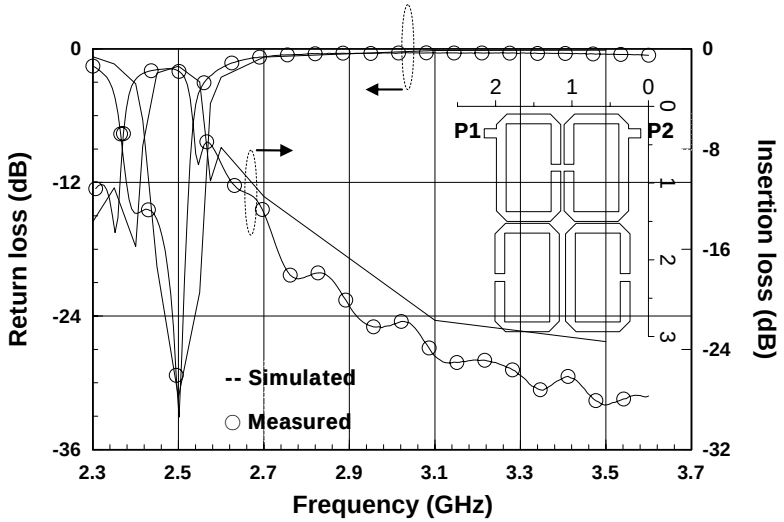

- IF sub-module – BPF1: measured and simulated result, with the pass band from 2.397 to 2.497 GHz and the rejection band from 3.353 to 3.453 GHz
- Insertion loss: > -2.3 dB
- Rejection: < -27 dB
- Layout size: 2 cm (W) * 2.9 cm (L)

Figure 3.2.2-1 measurement result of BPF1 of pass band from 3.403 to 3.453 GHz

To extract the external quality factor form the simulated S11 gets the geometry dimension of the ring.

To adjust the gap between the ring 1 and 2 (as well as the gap between ring 3 and 4) and another gap between the ring 2 and 3 meets designed coupling coefficients of M12 (as well as M34) and M23, respectively, due to the symmetrical structure of filter layout.

Figure 3.2.2-1 is the measurement and simulation result of BPF1 which has the layout size of 2 cm width and 2.9 cm length with the measured insertion loss greater than -2.3 dB from 2.397 to 2.497 GHz and the measured rejection less than -27 dB regarding to the band from 3.353 to 3.453 GHz.

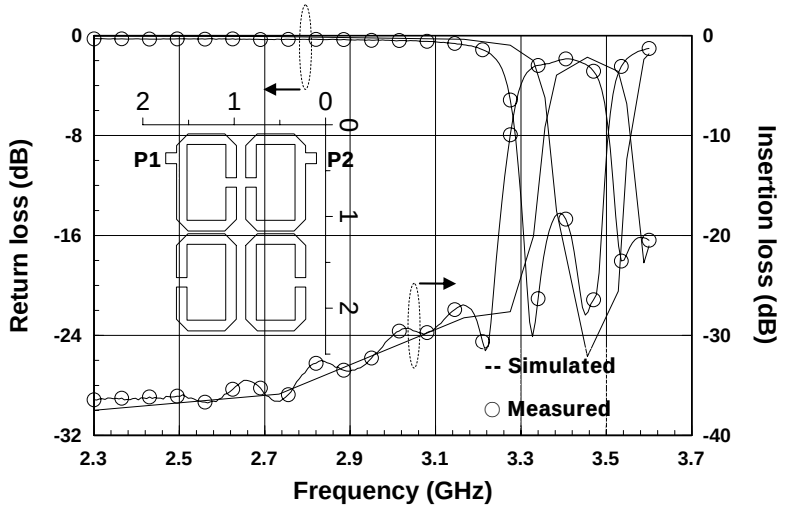

- IF sub-module – BPF2: measured and simulated result, with the pass band from 3.353 to 3.453 GHz and the rejection band from 2.397 to 2.497 GHz
- Insertion loss: > -2.9 dB
- Rejection: < -26 dB
- Layout size: 1.7 cm (W) * 2.2 cm (L)

Figure 3.2.2-2 Measurement result of BPF2 of pass band from 2.397 to 2.497 GHz

Figure 3.2.2-2 is the measurement and simulation result of BPF2 which has the layout size of 1.7 cm width and 2.2 cm length with the measured insertion loss greater than -2.9 dB from 3.353 to 3.453 GHz and the measured rejection less than -26 dB regarding to the band from 2.397 to 2.497 GHz.

Table 3-2 presents the gain budget analysis of the IF sub-module under the TX and RX mode, respectively, based on the gain or loss from the data sheet of discrete components and simulated results.

Sub-module: IF	U1 / U2 - HMC435MS8G / HITTITE							
	U3 / U4 - HMC168C8 / HITTITE					DIPLEXER1		
Operation mode: TX mode	U1 / U2	U3	BPF1	BA3	BA6	HPF1	LPF1	IF output port
Gain / Loss (dB): Design goal	-0.50	-13.00	-4.00	14.00	0.00	-1.50	-1.50	-0.50
Signals of ELEMENT A (dBm) per stage injected 13 dBm from 2.397 to 2.497 GHz	12.50	-0.50	-4.50	9.50	9.50	8.00		7.50
Signals of ELEMENT B (dBm) per stage injected 13 dBm from 2.397 to 2.497 GHz	12.50						11.00	10.50
						DIPLEXER2		
Operation mode: RX mode	U1 / U2	U4	BPF2	BA2	BA1	HPF1	LPF1	IF input port
Gain / Loss (dB): Design goal	-0.50	-14.00	-4.00	14.00	14.00	-1.50	-1.50	-0.50
Received PW of ELEMENT A (dBm) per stage injected -20 dBm during RF bnad	-12.50	-12.00	2.00	6.00	-8.00	-22.00		-20.50
Received PW of ELEMENT B (dBm) per stage injected -20 dBm during RF bnad	-22.50						-22.00	-20.50

Table 3-2 the gain budget analysis table of the IF sub-module

Per the up-side line-up analysis of Table 3-2 under the TX mode, the predicted TX power of ELEMENT A is 7.5 dBm and so is 10.5 dBm with respect to ELEMENT B.

Under the RX mode, in the down-side of Table 3-2, the assumed RX power of ELEMENT A is -12.5 dBm and so is -22.5 dBm to ELEMENT B

3.2.3 Measurement of IF sub-module

	ELEMENT A			ELEMENT B		
	Measurement	Analysis	Delta	Measurement	Analysis	Delta
TX power (dBm)	8.00	7.50	0.50	11.17	10.50	0.67
RX power (dBm)	-14.67	-12.50	-2.17	-22.67	-22.50	-0.17

Table 3-3 the consolidated table of TX and RX power measurement in the IF sub-module

Table 3-3 is the consolidated table of TX and RX power measurement compared with the performance predicted results shown in Table 3-2.

The line-up of the IF sub-module shell be modified to let the conversion gain relative to ELELMENT A and B be balanced under the TX or RX mode. The modification of line-up in the IF sub-module is mentioned in section 3-4 for details.

The delta value between the RX power measured under the TX and RX mode is the isolation between the TX and RX mode of ELEMENT A (as well as ELEMENT B).

The T/R isolation relative to ELEMENT A is 34.37 dBc shown in Graph 3-4 (a) and so is 37.16 dBc shown in Graph 3-4 (b) to ELEMENT B.

Both of them are dependent on the capability of T/R controlled switches of U1 and 2.

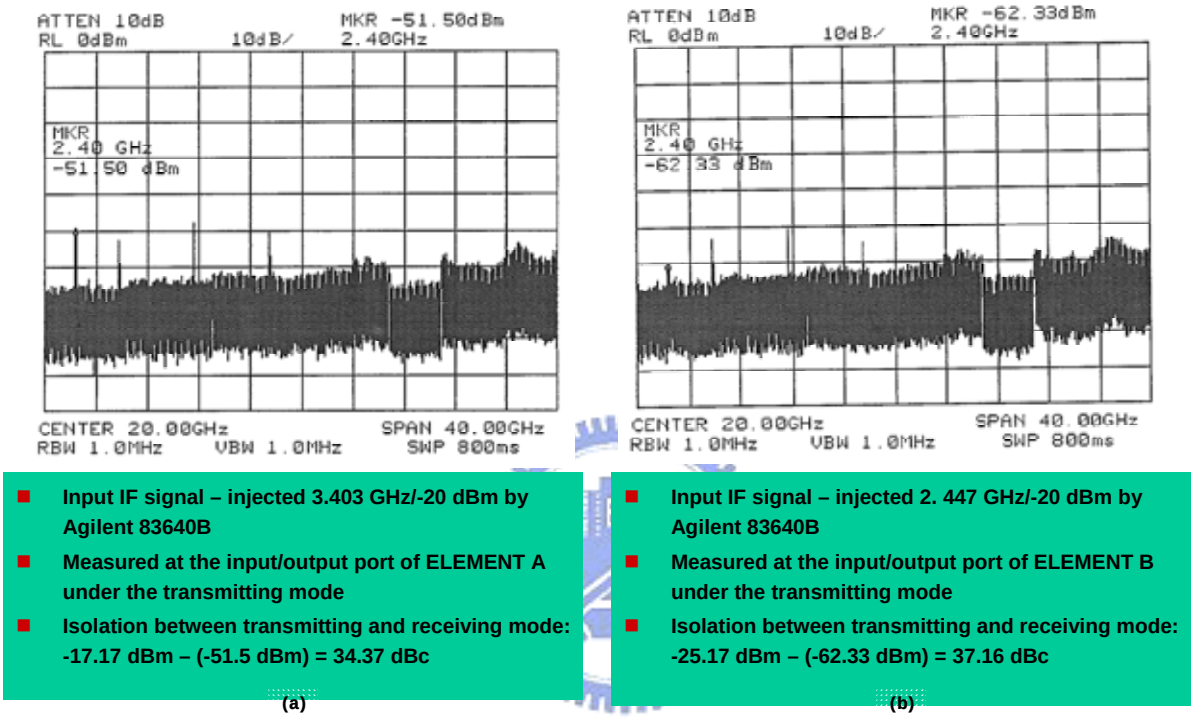

- Input IF signal – injected 3.403 GHz/-20 dBm by Agilent 83640B
- Measured at the input/output port of ELEMENT A under the transmitting mode
- Isolation between transmitting and receiving mode: -17.17 dBm – (-51.5 dBm) = 34.37 dBc

(a)

- Input IF signal – injected 2. 447 GHz/-20 dBm by Agilent 83640B
- Measured at the input/output port of ELEMENT B under the transmitting mode
- Isolation between transmitting and receiving mode: -25.17 dBm – (-62.33 dBm) = 37.16 dBc

(b)

Graph 3-4 the isolation between the TX and RX mode of (a) ELEMENT A (b) ELEMENT B in the IF sub-module

The delta value between the RX power measured at the input/output port of ELEMENT A (as well as ELEMENT B) and injected CW signals during the pass band of ELEMENT B (as well as ELEMENT A) is the element isolation of ELEMENT A (as well as ELEMENT B).

The element isolation relative to ELEMENT A is 33.5 dBc shown in Graph 3-5 (a) and so is 41.33 dBc shown in Graph 3-5 (b) regarding to ELEMENT B.

Both of them are based on the capability of diplexers of DIPLEXER1 and 2.

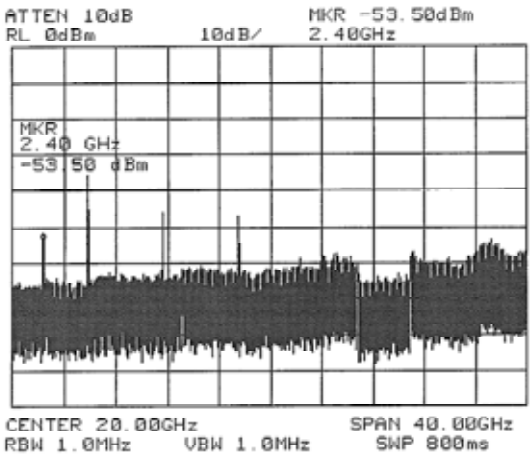

- Input IF signal – injected 2.447 GHz/-20 dBm by Agilent 83640B
- Measured at the input/output port of ELEMENT A under the receiving mode
- Isolation between ELEMENT A and B: -20 dBm – (-53.5 dBm) = 33.5 dBc

(a)

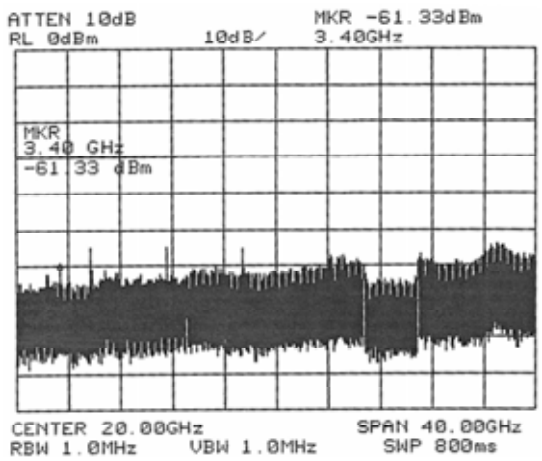

- Input IF signal – injected 3.403 GHz/-20 dBm by Agilent 83640B
- Measured at the input/output port of ELEMENT B under the receiving mode
- Isolation between ELEMENT A and B: -20 dBm – (-61.33 dBm) = 41.33 dBc

(b)

Graph 3-5 the isolation between ELEMENT A and B measured at the input/output port of (a) ELEMENT A (b) ELEMENT B

3.3 RF sub-module

With the considerations for usage bands of uplink and downlink and the channel isolation between the RF TX and RX path, the RF sub-module contains two parts which are

- TX sub-module of the detail block diagram shown in Figure 3-4 and the picture at the upper portion of Graph 3-6.

- RX sub-module shown in Figure 3-3 and the location below TX sub-module in Graph 3-6.

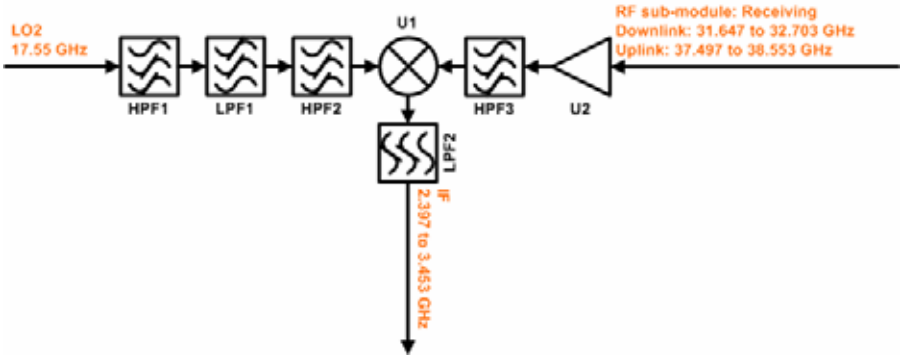

Figure 3-3 the block diagram of RX RF sub-module

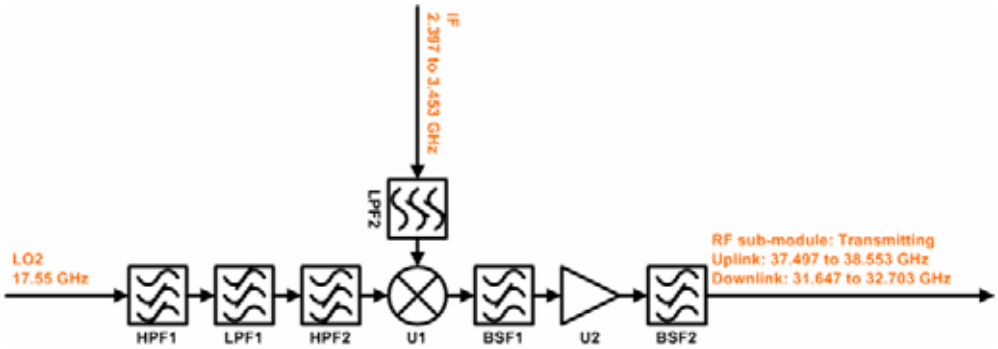

Figure 3-4 the block diagram of TX RF sub-module

In the TX path:

U1 in both sides is the sub-harmonically pumping mixer (SHPM) consisted of anti-parallel Schottky pair of DMK2308-0000 manufactured by SKYWORKS transferring IF signals from 2.397 to 3.453 GHz up to

- LSB mixing: the Ka lower frequency band from 31.647 to 32.703 GHz for RSU

- USB (Upper Side Band) mixing: the Ka higher frequency band from 37.497 to 38.553 GHz for OBU.

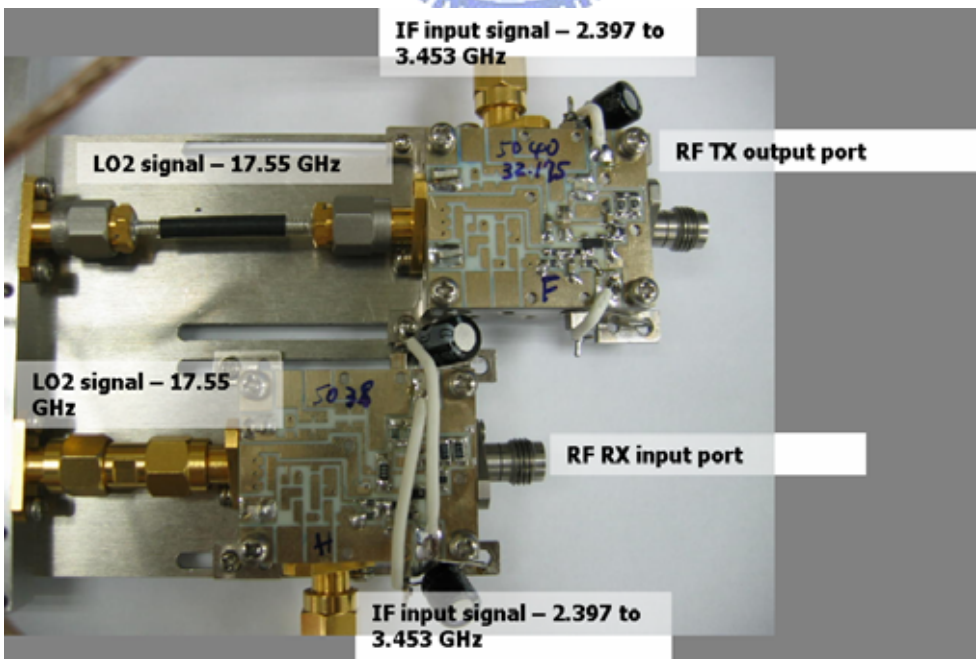

Graph 3-6 the top photograph view of RF sub-module

U2 is HMMC5040 which is the MMIC device manufactured by Agilent having following advantages

- High gain contributed by inside multiple stages of amplifier

- Inner matched network for the 50 OHM source and load system

to make it a cost effective alternative to hybrid (discrete-FET) amplifier.

Both of BSF 1 and 2 are the same design of the band stop filter (BSF) [6] to avoid the image spurious of RF signals leaking into the outside antenna port of the RX path.

Before the transmitting away form the TX antenna port, IF signals are going through the signal flowing path which is containing the up-conversion of U1, the filtering of BSF1 and 2 and the amplifying of U2.

In the RX path:

Components in the RX path are almost same as these ones in the TX sub-module, except

- MMIC LNA (Low Noise Amplifier) device of U2

- HPF3 between U1 and U2 for the signal isolation between RF signals and LO2 (as well as IF signals).

For considerations of electrical performances relative to the application of different RF operation bands, U2 is chosen as

- CHA2092b-99F manufactured by USM for the lower frequency band from 31.647 to 32.703 GHz

- HMMC5038 manufactured by Agilent for the higher band from 37.497 to 38.553 GHz.

Having been amplified by U2, received RF signals from the RX antenna port are frequency-conversed by the SHPM down to the IF frequency band for the IF sub-module.

Per the line-up analysis of Table 3-4 based on the gain or loss from the data sheet of discrete components and simulated results, the analyzed RF TX output power would be 2.08 dBm, if the injected power of IF signals is -2 dBm.

Sub-module: RF TX — U1 - Anti-parallel DMK2308-000 / SKYWORKS diode pair; U2 - HMMC-5040 / Agilent

	LPF2	U1	BSF1	U2	BSF2	RF TX output port
Gain / Loss (dB): Design goal	-2.00	-9.92	-2.50	22.00	-2.50	-1.00
IF signals (dBm) injected -2 dBm from 2.397 to 3.453 GHz	-4.00					
RF TX output power (dBm) per stage		-13.92	-16.42	5.58	3.08	2.08

Table 3-4 the gain budget analysis table of the RF TX sub-module

Per the line-up analysis of Table 3-5 based on the gain or loss from the data sheet of discrete components and simulated results, in the case of U2 being CHA2093b-99F, the received power of IF signals is -14.94 dBm and so will be -15.34 dBm regarding to another case of HMMC5038, if the input power of RF signals is -20 dBm.

Sub-module: RF RX — U1 - Anti-parallel DMK2308-000 / SKYWORKS diode pair; U2 - HMMC-5038 / Agilent (37.497 to 38.553 GHz); U2 - CHA2092b-99F / UMS (31.647 to 32.703 GHz)

U2: CHA2092b-99F	LPF2	U1	HPF3	U2	RF RX input port
Gain / Loss (dB): Design goal	-2.00	-12.34	-1.60	22.00	-1.00
RF signals (dBm) per stage injected -20 dBm from 31.647 to 32.703 GHz			-0.60	1.00	-21.00
IF received power (dBm) per stage	-14.94	-12.94			

U2: HMMC-5038	LPF2	U1	HPF3	U2	RF RX input port
Gain / Loss (dB): Design goal	-2.00	-13.84	-1.50	23.00	-1.00
RF signals (dBm) per stage injected -20 dBm from 37.497 to 38.553 GHz			0.50	2.00	-21.00
IF received power (dBm) per stage	-15.34	-13.34			

Table 3-5 the gain budget analysis table of the RF RX sub-module

3.3.1 Design of sub-harmonically pumped mixer (SHPM)

With the characteristic of wide usage band width regarding to the component design during the Ka frequency band, a topology of the low cost approach illustrated in [7] for the half input local frequency is proposed.

Based on the equation (3.1.3.5), for the applied voltage

$$V = V_{LO2} COS\omega_{LO2} t + V_{IF} COS\omega_{IF} t$$

, the current expression on the conductance consisted of the anti-parallel Schottky diode pair is

$$i = g(\frac{1}{2}V_{LO2}\omega_{LO2}t + \frac{1}{2}V_{IF}\omega_{IF}t) = A\cos(\omega_{LO2}t) + B\cos(\omega_{IF}t) + C\cos(3\omega_{LO2}t)$$
$$+ D\cos(5\omega_{LO2}t) + E\cos[(2\omega_{LO2} + \omega_{IF})t]$$
$$+ F\cos[(2\omega_{LO2} - \omega_{IF})t] + G\cos[(4\omega_{LO2} + \omega_{IF})t]$$
$$+ H\cos[(4\omega_{LO2} - \omega_{IF})t] + ...$$

- Equation (3.3.1.1)

It can be seen that the total current only contains frequency terms $mf_{LO2} \pm nf_{IF}$ where $m+n$ is an odd integer; i.e., $m+n = 1,3,5,....$

To the terms of $E\cos[(2\omega_{LO2} + \omega_{IF})t]$ and $F\cos[(2\omega_{LO2} - \omega_{IF})t]$, there are existing mixing terms relative to IF signals and 2*LO2. The wanted conversed-signal would be filtered by the simple structure as shown as Figure 3.3.1-1.

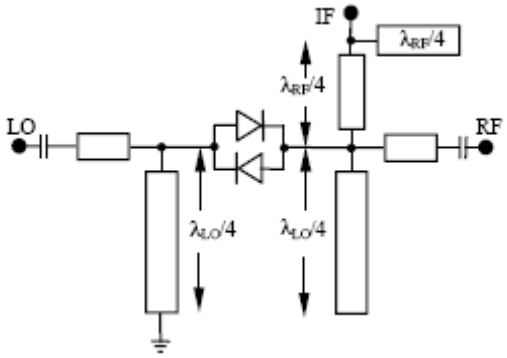

Figure 3.3.1-1 the design scheme of SHPM

With these following filtering circuitries

- The shunt short-stub designed for the quarter wave-length of LO signal, which connected to the input port of local signal, to reject the 2*LO signal, or approximately the RF signal and provide the return path of IF signal

- The shunt open-stub designed for the quarter wave-length of LO signal, which is placed at the output diode pair side, to suppress the LO signal

- The RF rejection choke composed of the quarter wave-length long open-stub which is designed at the RF frequency and placed at the IF port, and the quarter wave-length transmission line which is designed at RF frequency and located between the IF port and the output diode pair side

, and the block capacitor for IF signals on the RF port. It can obtain the RF signal in term of 2*LO+IF, or 2*LO-IF, in purpose of the frequency conversion function in the RF sub-module.

The following figure of 3.3.1-2 is the realized layout daring of SHPM sub-block assembled on the Al2O3 substrate.

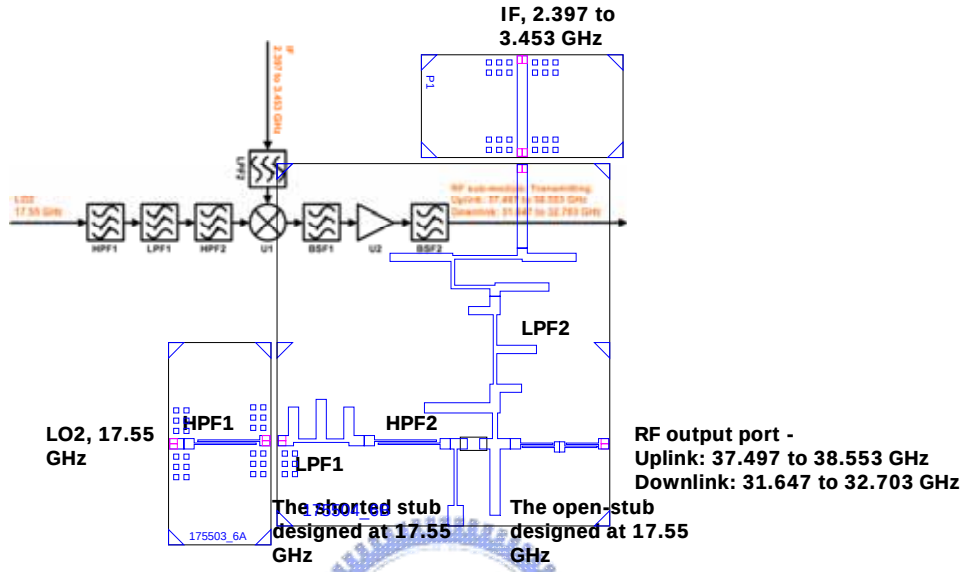

Figure 3.3.1-2 the layout drawing of SHPM sub-block

Figure 3.3.1-3 (a) presents the simulation result of BPF, which is composed of HPF1 and 2, and LPF1, between the input port of LO2 and the input diode pair side for the suppression of RF and IF signal.

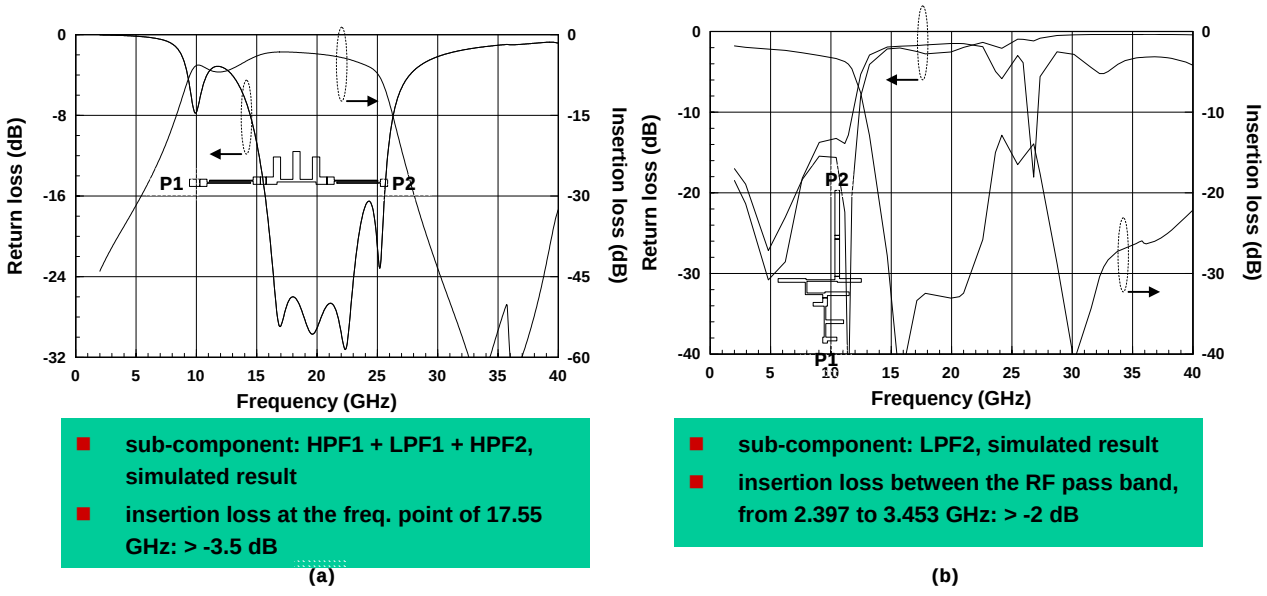

Figure 3.3.1-3 (a) the simulation result of BPF composed of HPF1 and 2, and LPF1 (b) the

simulation result of LPF2

Figure 3.3.1-3 (b) is the simulation result of LPF2 between the input port of IF and the output diode pair side in order to the rejection of both LO2 and RF signals.

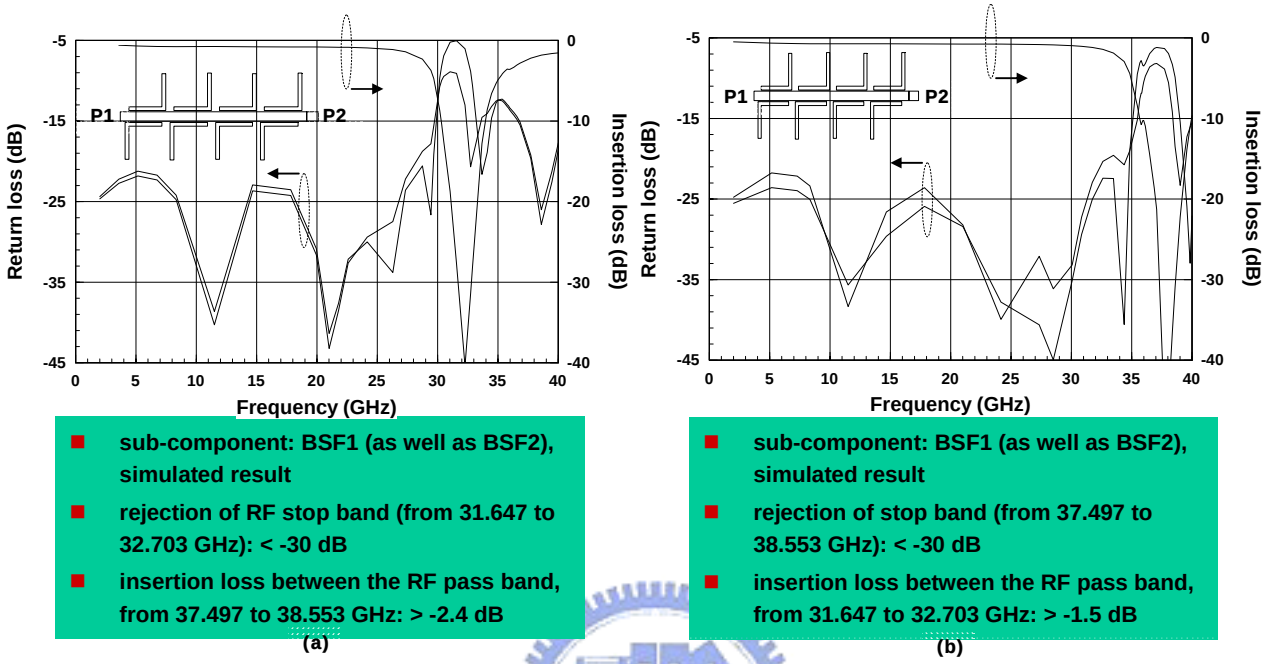

Figure 3.3.1-4 the simulation result of band stop filter of BSF1 (as well as BSF2) (a) during the downlink frequency band from 31.647 to 32.703 GHz (b) during the uplink frequency band from 37.497 to 38.553 GHz for the rejection of mixed output image signals

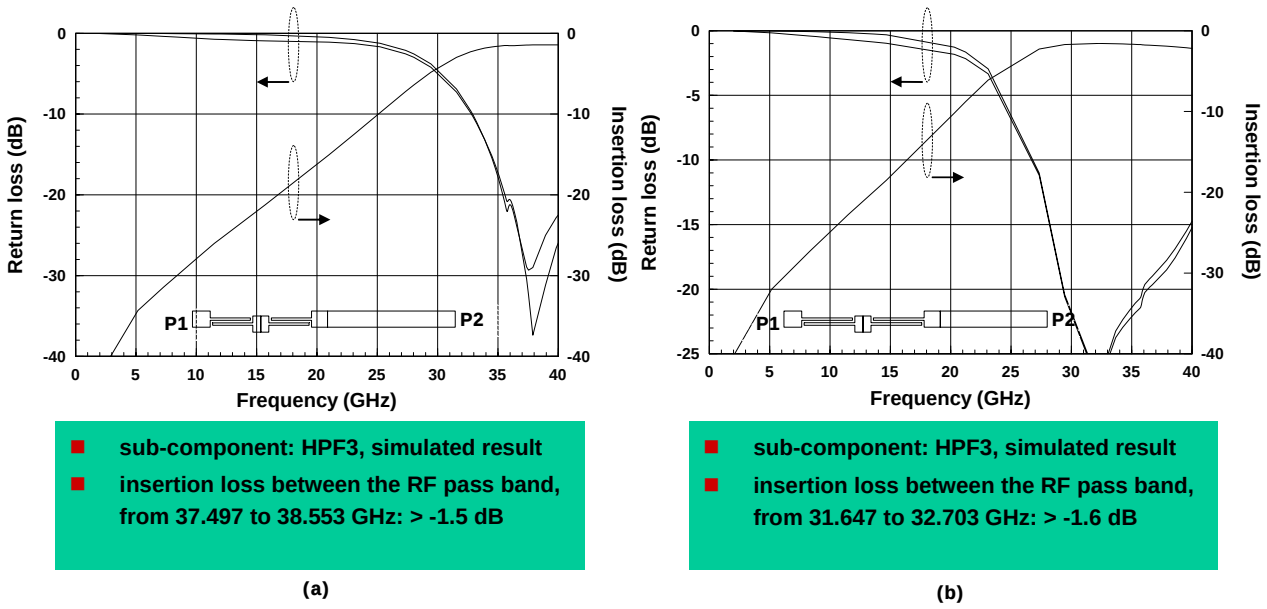

Figure 3.3.1-5 the simulation result of high pass filter of HPF3 (a) during the downlink frequency band from 31.647 to 32.703 GHz (b) during the uplink frequency band from 37.497

to 38.55 GHz for the suppression of LO2 and IF signals

With simulation results of sub-components shown in the Figure 3.3.1-3 and

- The band stop filter of BSF1 for the RF TX sub-module with simulation results shown in Figure 3.3.1-4

- The high pass filter of HPF3 for the RF RX sub-module with simulation results shown in Figure 3.3.1-5

, the simulated integrated performances of SHPM are shown in Figure 3.3.1-6 for the frequency up-conversion and in Figure 3.3.1-7 for the down-conversion, respectively.

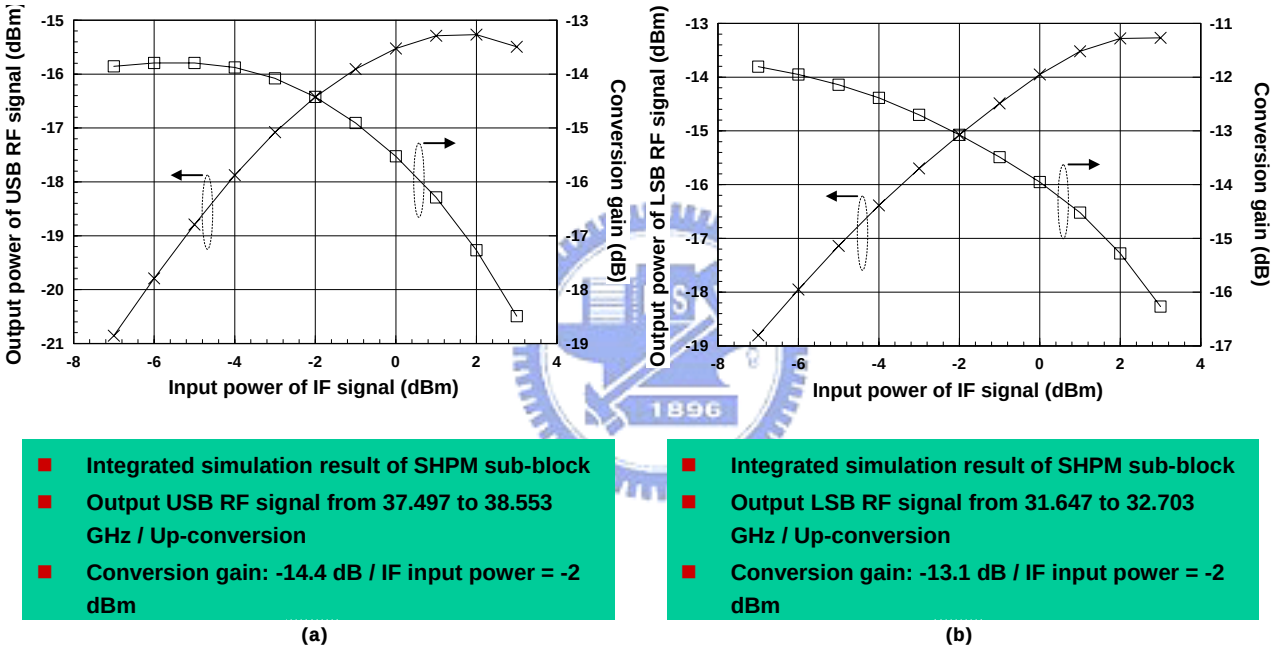

Figure 3.3.1-6 the simulated performance of integrated up-conversion gain: (a) output USB RF signals (b) output LSB RF signals

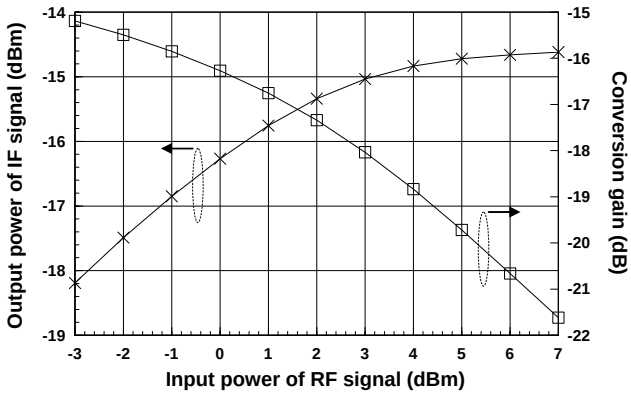

- Integrated simulation result of SHPM sub-block
- Injected RF signal from 37.497 to 38.553 GHz / Down-conversion
- Conversion gain: -17.34 dB / Input power of RF signal = 2 dBm

(a)

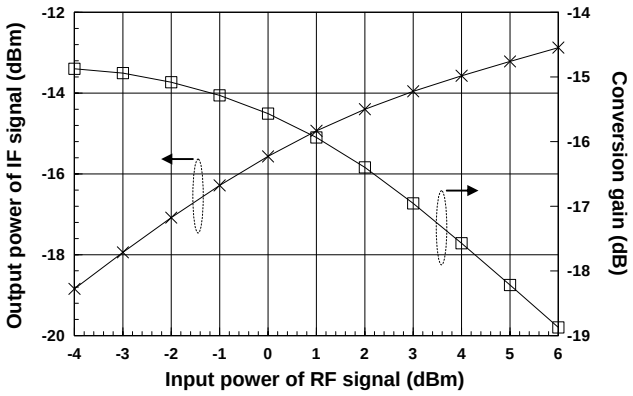

- Integrated simulation result of SHPM sub-block
- Injected RF signal from 31.647 to 32.703 GHz / Down-conversion
- Conversion gain: -15.94 dB / Input power of RF signal = 1 dBm

(b)

Figure 3.3.1-7 the simulated performance of integrated down-conversion gain: (a) injected RF signal from 37.497 to 38.553 GHz (b) injected RF signal from 31.647 to 32.703 GHz

	Frequency-sifted of ELEMENT A (3.353 to 3.453 GHz)			ELEMENT B (2.397 to 2.447 GHz)		
	Measurement	Analysis	Delta	Measurement	Analysis	Delta
TX conversion gain (dB) (LSB RF band from 31.647 to 32.703 GHz)	-9.67	-13.07	3.40	-12.67	-13.07	0.40
TX conversion gain (dB) (USB RF band from 37.497 to 38.553 GHz)	-11.67	-14.42	2.75	-11.5	-14.42	2.92
RX conversion gain (dB) (injected RF signal from 31.647 to 32.703 GHz)	-9.67	-15.94	6.27	-10.83	-15.94	5.11
RX conversion gain (dB) (injected RF signal from 37.497 to 38.553 GHz)	-9.83	-17.34	7.51	-9.33	-17.34	8.01

Table 3.3.1-1 the consolidated conclusion table of SHPM sub-block

From the consolidated conclusion table of Table 3.3.1-1, the RX conversion gain has the larger delta variation from 5.11 to 8.01 dB between the assumption of gain budget analysis and the measurement. It shall be the reasons that

- The assembled diode pair has the lower junction capacitor of zero biasing than the typical setting value in the simulation file

- The loss of sub-components of the SHPM block is less than the value of simulated result.

3.3.2 Measurement of RF sub-module

Table 3-6 is the consolidated table of TX and RX conversion gain measurement compared with the predicted performance shown in Table 3-4 and 3-5 for TX and RX sub-module, respectively.

	Frequency-sifted of ELEMENT A (3.353 to 3.453 GHz)			ELEMENT B (2.397 to 2.447 GHz)		
	Measurement	Analysis	Delta	Measurement	Analysis	Delta
TX conversion gain (dB) (LSB RF band from 31.647 to 32.703 GHz)	8.83	4.08	4.75	9.83	4.08	5.75
TX conversion gain (dB) (USB RF band from 37.497 to 38.553 GHz)	8.33	4.08	4.25	4.33	4.08	0.25
RX conversion gain (dB) (injected RF signal from 31.647 to 32.703 GHz)	6.67	5.06	1.61	6.50	5.06	1.44
RX conversion gain (dB) (injected RF signal from 37.497 to 38.553 GHz)	5.50	4.66	0.84	7.00	4.66	2.34

Table 3-6 the consolidated table of TX and RX conversion gain of RF sub-module

Regarding to the TX conversion gain with the larger delta value between the measurement and the analysis, it shell be the reason that the loss of passive sub-components in the TX path is less than the value of simulated result.

Up-conversed RF signals in the frequency spectrum are given by Graph 3-7 to present that the worst case of USB spurious labeled as number three is the product contributed by LO2 and 2*IF in the left side graph, as well as the LSB spurious labeled as number three in the right side.

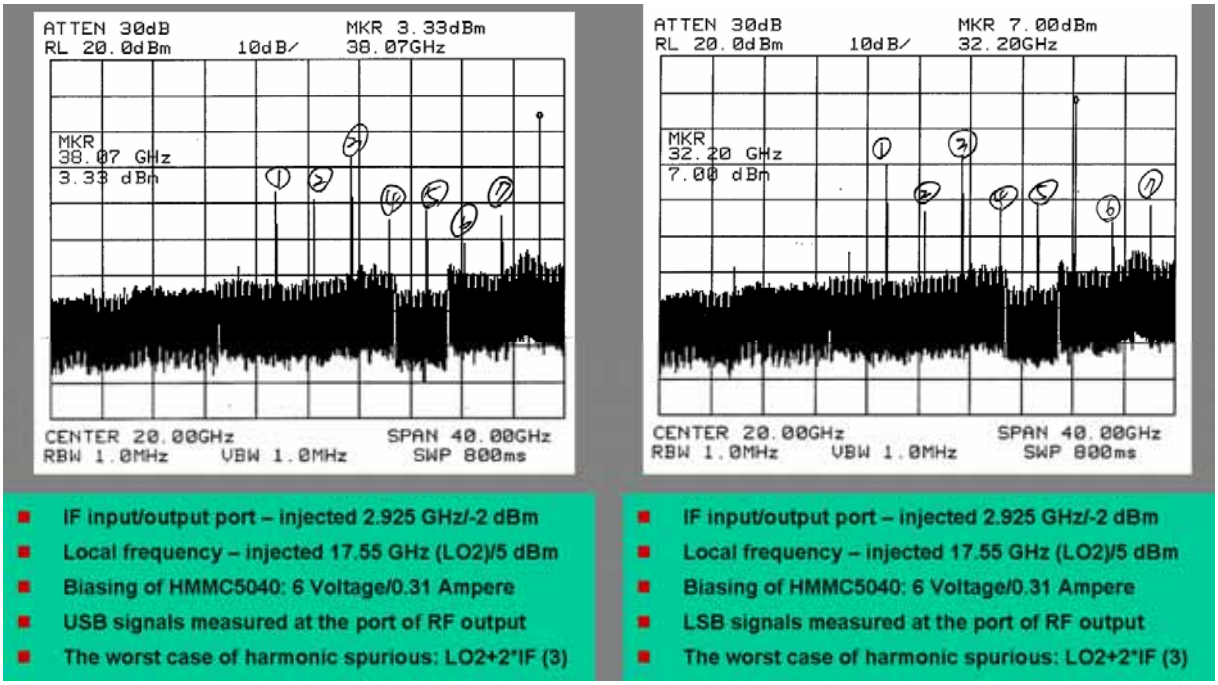

Graph 3-7 the output TX spurious measured data of RF TX sub-module

Down-conversed IF signals in the frequency spectrum are given by Graph 3-8 to present that the worst case of RX spurious labeled as number five is the leaked RF signal in the left side graph, if the injected power of RF signal is -20 dBm at 38.025 GHz.

In the right side, the worst case of RX spurious marked as number four is the leaked LO2 signal (17.55 GHz), if the injected power of RF signal is -20 dBm at 32.175 GHz.

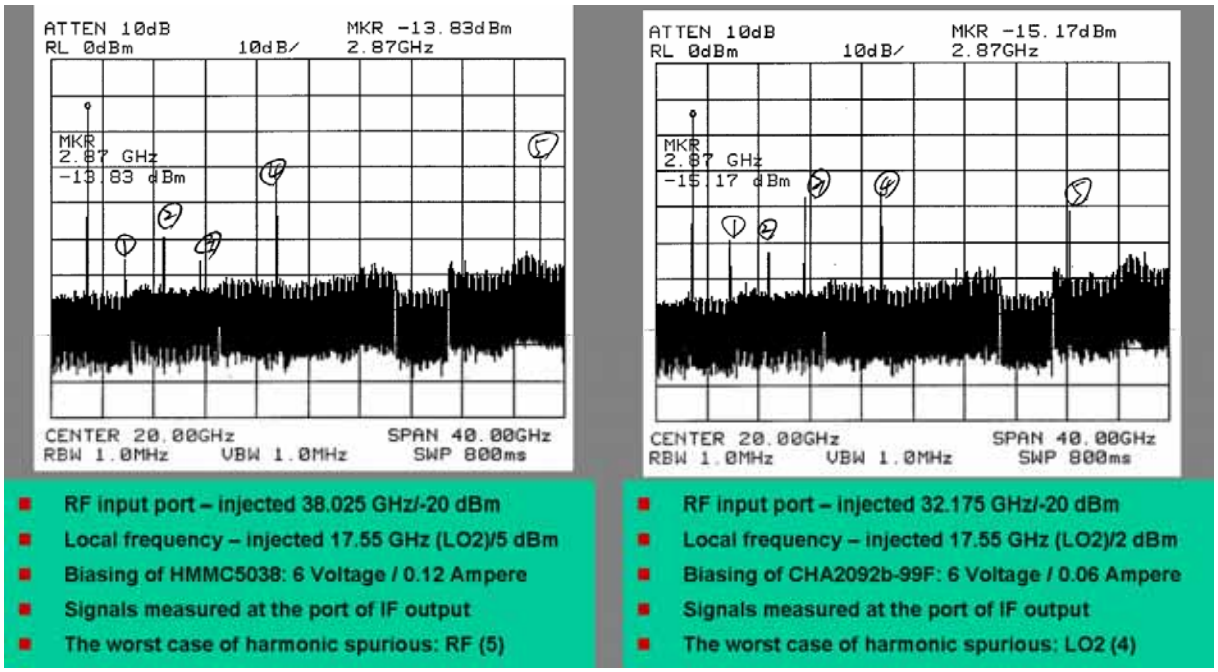

Graph 3-8 the received spurious measured data of RF TX sub-module

3.4 Modification of line-up

Having verified the local frequency, IF and RF sub-module as mentioned in section 3.1, 3.2 and 3.3, respectively, it needs to modify the line-up of sub-module for the optimization of the systematical performance.

U1 / U2 - HMC435MS8G / HITTITE U3 / U4 - HMC168C8 / HITTITE	IF sub-module								RF sub-module	
						DIPLEXER1				
Operation mode: TX mode	U1 / U2	U3	BPF1	BA3	BA6	HPF1	LPF1	IF output port	up-conversed USB gain	up-conversed LSB gain
Gain / Loss (dB): Design goal	-0.50	-13.00	-4.00	17.00	0.00	-1.50		-0.50		
TX power of ELEMENT A (dBm) per stage injected 0 dBm IF signals from 2.397 to 2.497 0.00 GHz	-0.50	-13.50	-17.50	-0.50	-0.50	-2.00		-2.50	8.33	8.83
TX power of RF signals (dBm) per stage RSU, RF operation band from 31.647 to 31.747 GHz										6.33
TX power of RF signals (dBm) per stage OBU, RF operation band from 38.453 to 38.553 GHz									5.83	
	U1 / U2						LPF1	IF output port	up-conversed USB gain	up-conversed LSB gain
Gain / Loss (dB): Design goal	-0.50						-1.50	-0.50		
TX power of ELEMENT B (dBm) per stage injected 0 dBm IF signals from 2.397 to 2.497 0.00 GHz	-0.50						-2.00	-2.50	4.33	9.83
TX power of RF signals (dBm) per stage RSU, RF operation band from 32.603 to 32.703 GHz										7.33
TX power of RF signals (dBm) per stage OBU, RF operation band from 37.497 to 37.597 GHz									1.83	

Table 3.4-1 the modified gain budget table of the whole TX path in OBU and RSU

According to measured results in sub-modules, Table 3.4-1 is the modified gain budget table of the whole TX path in OBU and RSU in purpose of the equal path gain with respect to both of ELEMENT A and B in the IF sub-module.

Replacing BA3 with another amplifier of ERA-3SM which is manufactured by MINI-CIRCUITS with the higher gain of 17 dB than ERA-2SM, the conversion gain of IF sub-module is updated to -2.5 dB regarding to both of ELEMENT A and B without doing any changes of local frequency and RF sub-module; if the injected power of IF signals is 0 dBm.

U1 / U2 - HMC435MS8G / HITTITE U3 / U4 - HMC168C8 / HITTITE		IF sub-module								RF sub-module	
							DIPLEXER2				
Operation mode: RX mode		U1 / U2	U4	BPF2	BA2	BA1	HPF1	LPF1	IF input port	down-conversed gain	down-conversed gain
Gain / Loss (dB): Design goal		-0.50	-14.00	-4.00	0.00	14.00	-1.50		-0.50	6.67	5.50
RX power of ELEMENT A (dBm) per stage RSU, injected -20 dBm RF signals from 38.453 to 38.553 GHz	-1.00	-21.00	-20.50	-6.50	-2.50	-2.50	-16.50		-15.00		-14.50
RX power of ELEMENT A (dBm) per stage OBU, injected -20 dBm RF signals from 31.647 to 31.747 GHz	0.17	-19.83	-19.33	-5.33	-1.33	-1.33	-15.33		-13.83	-13.33	
		U1 / U2						LPF1	IF input port	down-conversed gain	down-conversed gain
Gain / Loss (dB): Design goal		-0.50						-4.50	-0.50	6.50	7.00
RX power of ELEMENT B (dBm) per stage RSU, injected -20 dBm RF signals from 37.497 to 37.597 GHz	1.50	-18.50						-18.00	-13.50		-13.00
RX power of ELEMENT B (dBm) per stage OBU, injected -20 dBm RF signals from 32.603 to 32.703 GHz	1.00	-19.00						-18.50	-14.00	-13.50	

Table 3.4-2 the modified gain budget table of the whole RX path in OBU and RSU

Table 3.4-2 is the modified gain budget table of the whole RX path in OBU and RSU. If the injected power level of RF signal is -20 dBm, change notes for the updated RX path during the IF sub-module are

- It removes the gain amplifier of BA2 and connects the path gap with the coupling capacitor of 100 pF for ELEMENT A

- Add one attenuator of 3 dB between LPF1 and the IF input port with respect to ELEMENT B

without modifying the local frequency and RF sub-module.

CHAPTER 4 INTGRATED MEASUREMENT

The following several sections are the detail description of test items shown as below

4.1 Output transmitting power

4.2 Receiving power of down-conversion

4.3 Noise figure

4.4 Link test

, including in the guide line test procedure, the testing setup and the graph of measurement results.

4.1 Output transmitting power

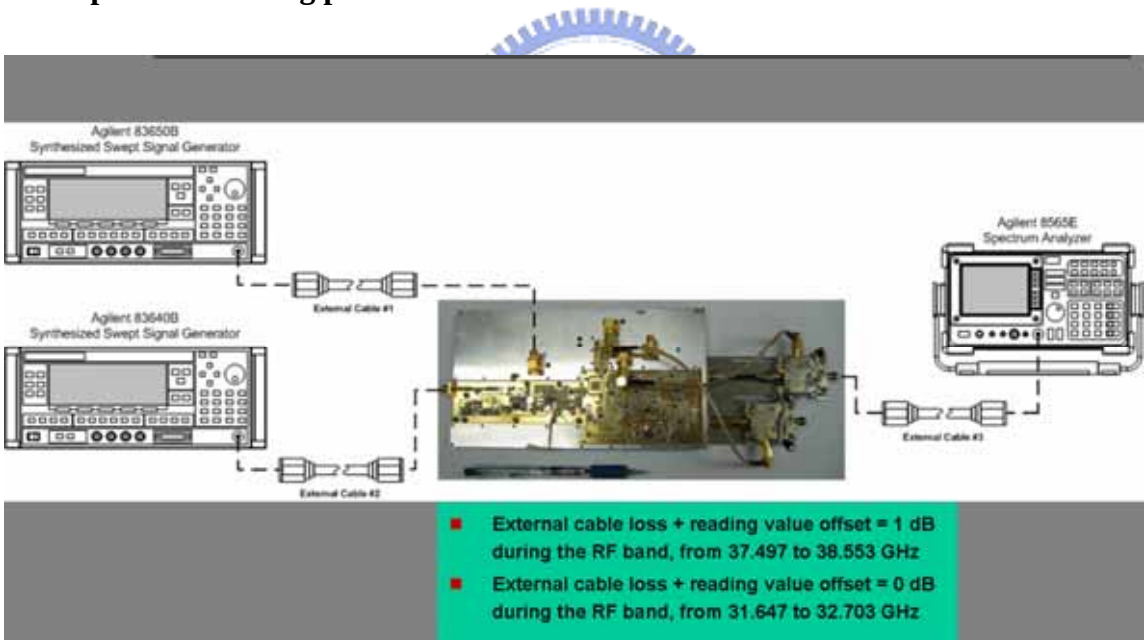

Figure 4-1 the test setup of output TX power measurement

The test procedure is shown as below and referred to Figure 4-1 for the test setup.

- Use the power sensor of Agilent 8487A and the power meter of Agilent E4418B to do the power calibration of the cable loss in the external cable #3 and of the power reading value on the spectrum analyzer, Agilent 8565E, during the TX RF frequency band.

- The synthesized swept signal generator of Agilent 83640B provides the 81.25 MHz CW

signal of the injected power being 0 dBm via the external cable #2 to be the reference signal of the local frequency sub-module.

- Use Agilent 8487A and E4418B to do the power calibration of the cable loss in the external cable #1 and of the power reading value on the synthesized swept signal generator, Agilent 83650B, during the IF frequency band in order to letting the excited power at the connected port of ELEMENT A (as well as ELEMENT B) be 0 dBm.

- After setting the IF sub-module under the TX mode. It applies calibrated CW signals which are from 2.397 to 2.497 GHz with 10 MHz frequency step and generated by Agilent 83650B at the connected port of ELEMENT A (as well as ELEMENT B).

- To link the connections as shown in Figure 4-1 and turn the DC supply feed on obtains serial measured values of output TX power on Agilent 8565E.

With the summarized 0 dB offset of the external cable loss and the reading value on equipments, the output TX conversion gain is 6.5 dB as shown in Graph 4-1 relative to ELEMENT B in RSU and 4.67 dB as shown in Graph 4-2 to ELEMENT A.

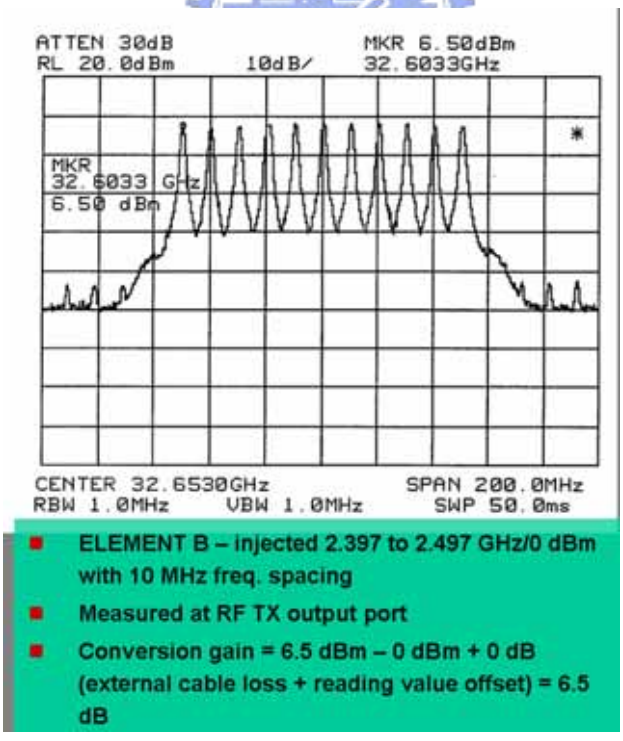

Graph 4-1 the measured TX output power of RSU – ELEMENT B

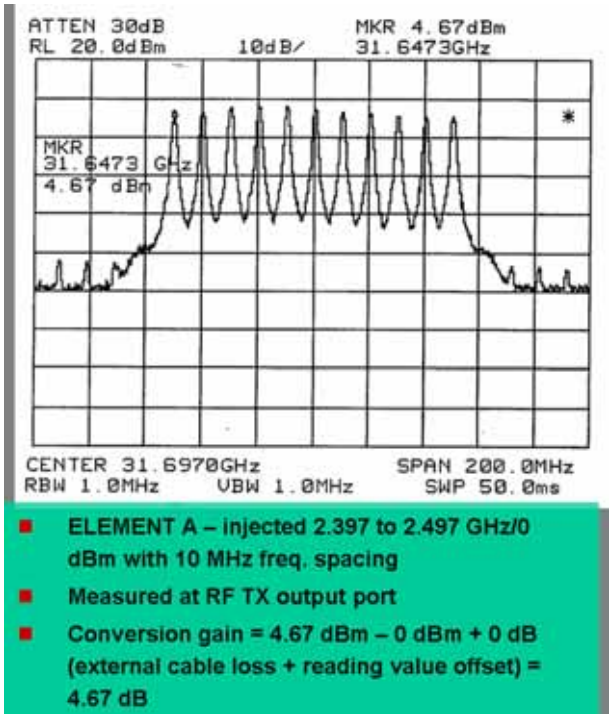

Graph 4-2 the measured TX output power of RSU – ELEMENT A

With the summarized 1 dB offset of the external cable loss and the reading value on equipments, the output TX conversion gain is 1.17 dB as shown in Graph 4-3 relative to ELEMENT B in OBU and 3.17 dB as shown in Graph 4-4 to ELEMENT A.

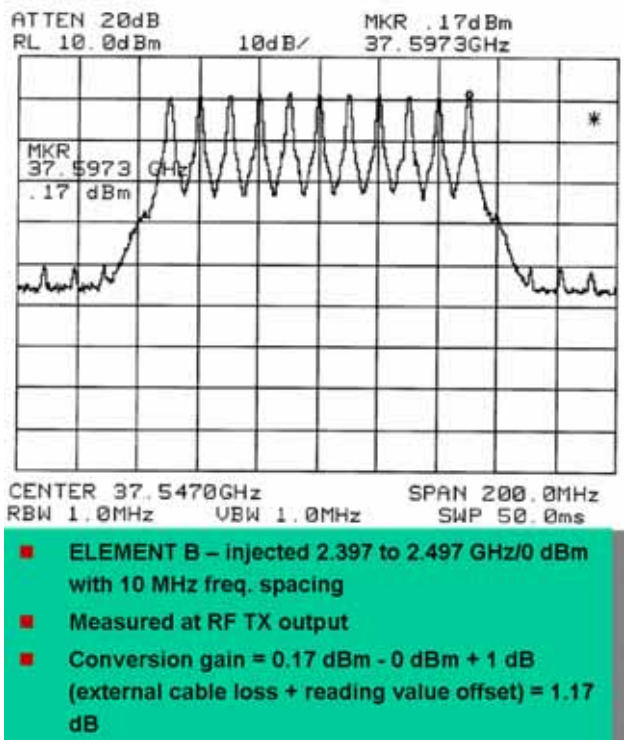

Graph 4-3 the measured TX output power of OBU – ELEMENT B

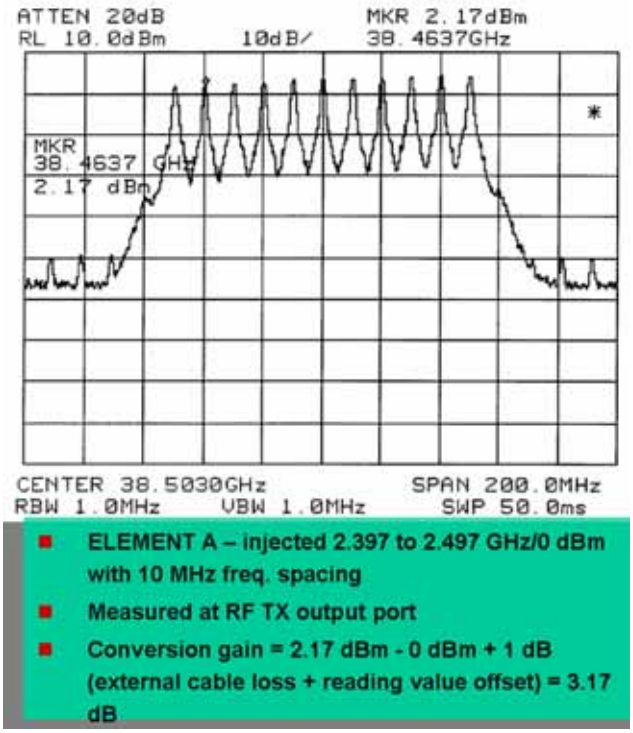

Graph 4-4 the measured TX output power of OBU – ELEMENT A

4.2 Receiving power of down-conversion

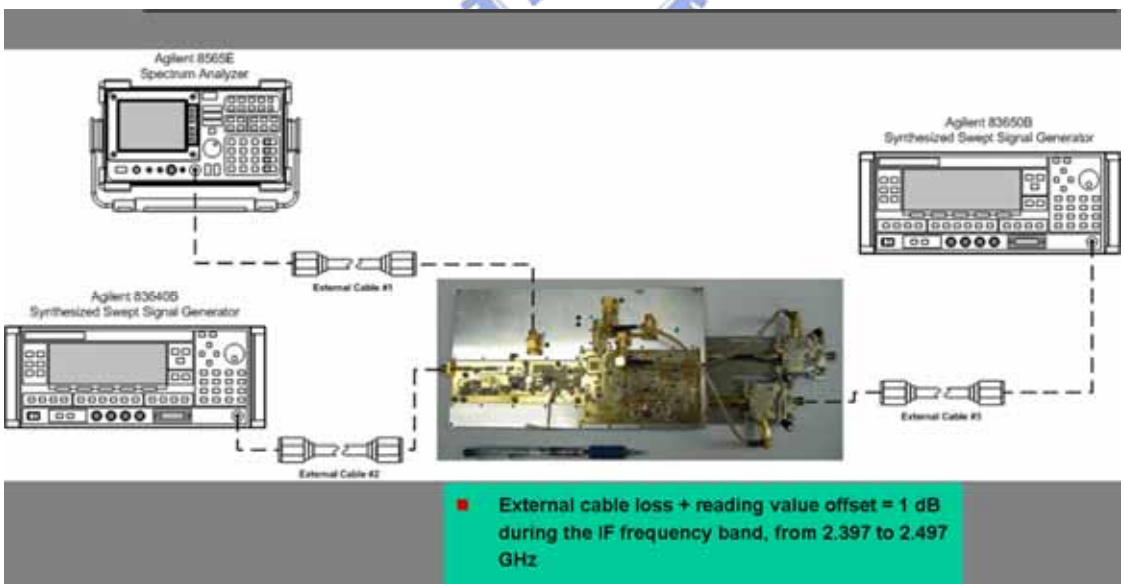

Figure 4-2 test setup of the measurement for the RX power of down-conversion

The test procedure is shown as below and referred to Figure 4-2 for the test setup.

- Use Agilent 8487A and E4418B to do the power calibration of the cable loss in the

external cable #1 and of the power reading value on Agilent 8565E during the RX IF frequency band.

- Agilent 83640B provides the 81.25 MHz CW signal of the injected power being 0 dBm via the external cable #2 to be the reference signal of the local frequency sub-module.

- Use Agilent 8487A and E4418B to do the power calibration of the cable loss in the external cable #3 and of the power reading value on Agilent 83650B during the RF frequency band in order to letting the injected power at the RF input port of RF RX sub-module be -20 dBm.

- It applies calibrated CW signals which are from 37.497 to 38.553 GHz with 10 MHz frequency step for RSU (as well as from 31.647 to 32.703 GHz for OBU) and generated by Agilent 83650B at the RF input port of RF RX sub-module.

- To link the connections as shown in Figure 4-2 and turn the DC supply feed on obtains serial measured values of the received IF power on Agilent 8565E.

With the summarized 1 dB offset of the external cable loss and the reading value on equipments, the RX conversion gain is -1.5 dB as shown in Graph 4-5 relative to ELEMENT B in RSU and -2.17 dB as shown in Graph 4-6 to ELEMENT A.

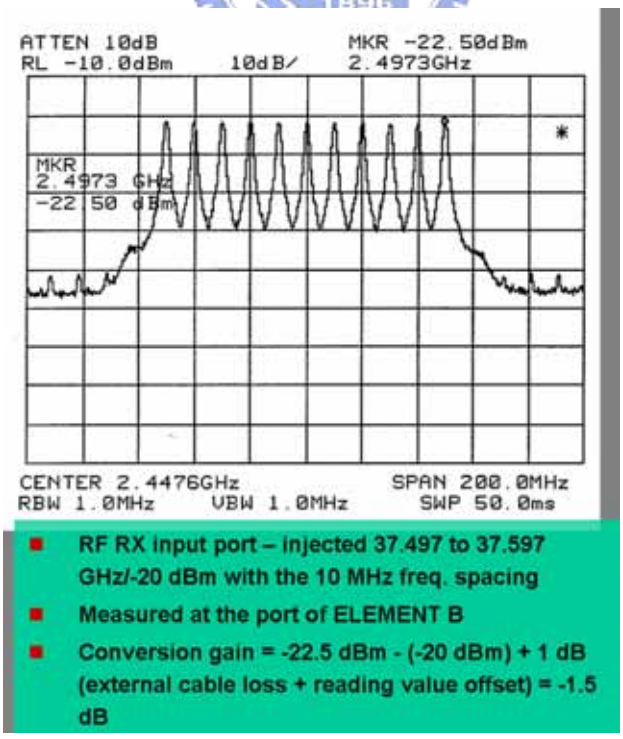

Graph 4-5 the measured down-conversion RX power of RSU – ELEMENT B

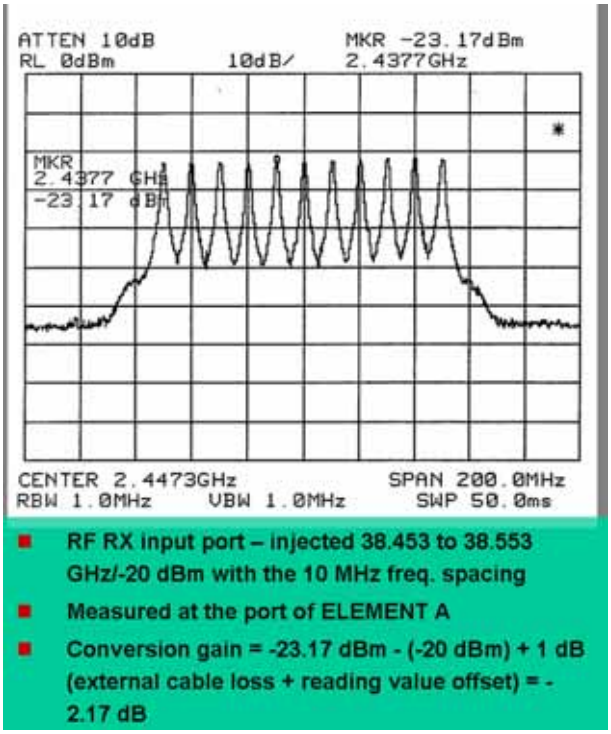

Graph 4-6 the measured down-conversion RX power of RSU – ELEMENT A

With the summarized 1 dB offset of the external cable loss and the reading value on equipments, the RX conversion gain is 2 dB as shown in Graph 4-7 relative to ELEMENT B in OBU and 2.5 dB as shown in Graph 4-8 to ELEMENT A.

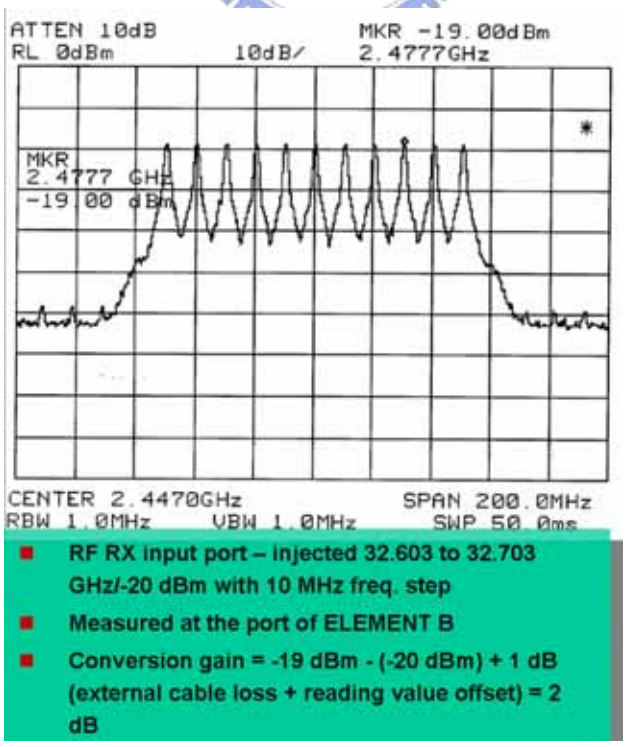

Graph 4-7 the measured down-conversion RX power of OBU – ELEMENT B

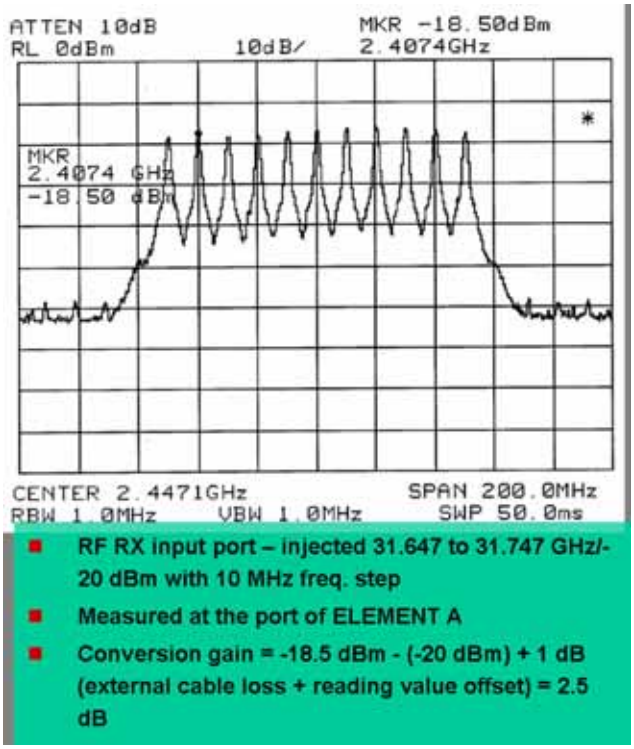

Graph 4-8 the measured down-conversion RX power of OBU – ELEMENT A

4.3 Noise figure

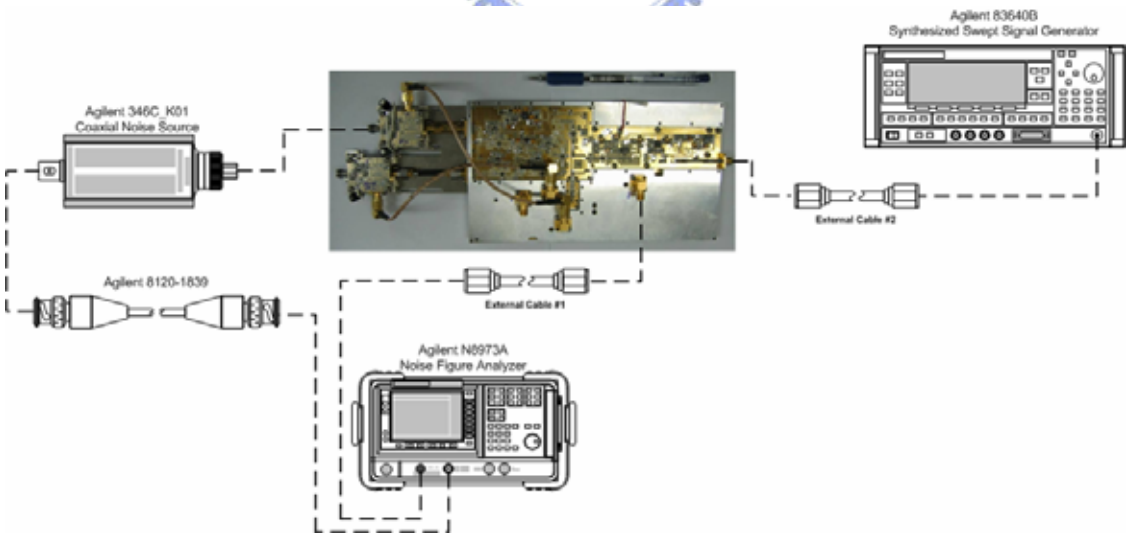

Figure 4-3 the test setup of noise figure measurement

The test procedure is shown as below and referred to Figure 4-3 for the test setup.

- Having keyed in the ENR data which is printed on the coaxial noise source of Agilent 346C_K01 during RF frequency band into the ENR table on the noise figure analyzer of Agilent

N8973A, press the key of “Calibrate” to do the calibration of noise figure for the reference plane between the external cable #1 and the output port of the noise source.

- Agilent 83640B provides the 81.25 MHz CW signal of the injected power being 0 dBm via the external cable #2 to be the reference signal of the local frequency sub-module.

- Set the IF-sub-module under the RX mode.

- Having linked the connections as shown in Figure 4-3 and turned the DC supply feed on, the noise figure value is measured on Agilent N8973A in the format of rectangular table.

The noise figure measured at the connected port of ELEMENT B in RSU is less than 9.8 dB shown in Graph 4-9 and less than 8.8 dB shown in Graph 4-11 to ELEMENT A.

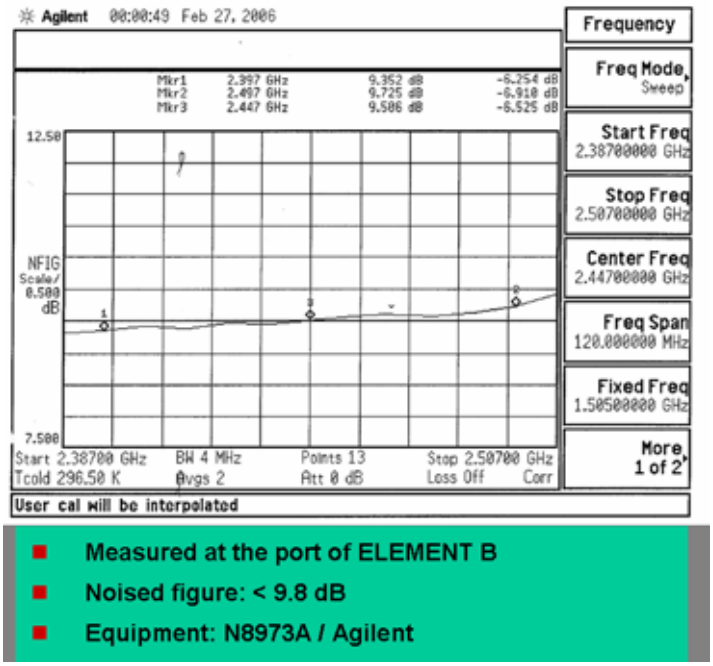

Graph 4-9 measured noise figure of RSU – ELEMENT B

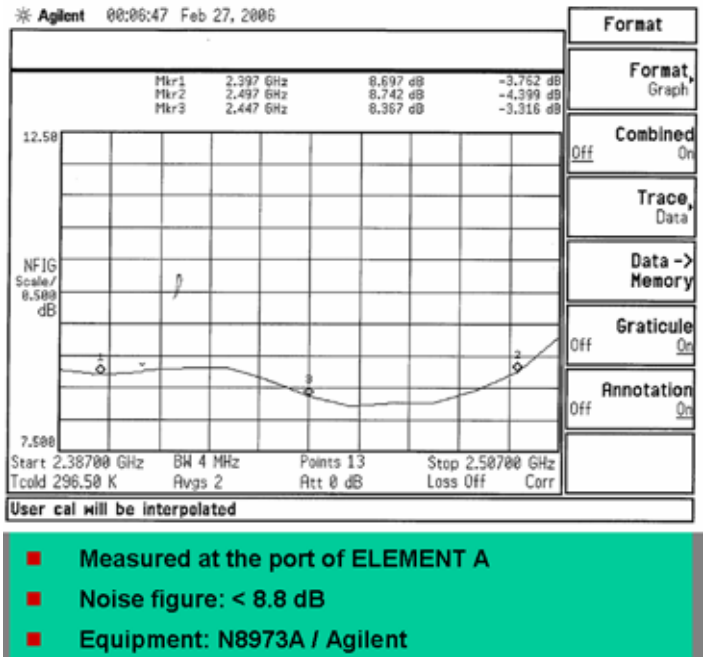

Graph 4-10 measured noise figure of RSU – ELEMENT A

The noise figure measured at the connected port of ELEMENT B in OBU is less than 7.5 dB as shown as Graph 4-11 and less than 7.4 dB as shown as Graph 4-12 to ELEMENT A.

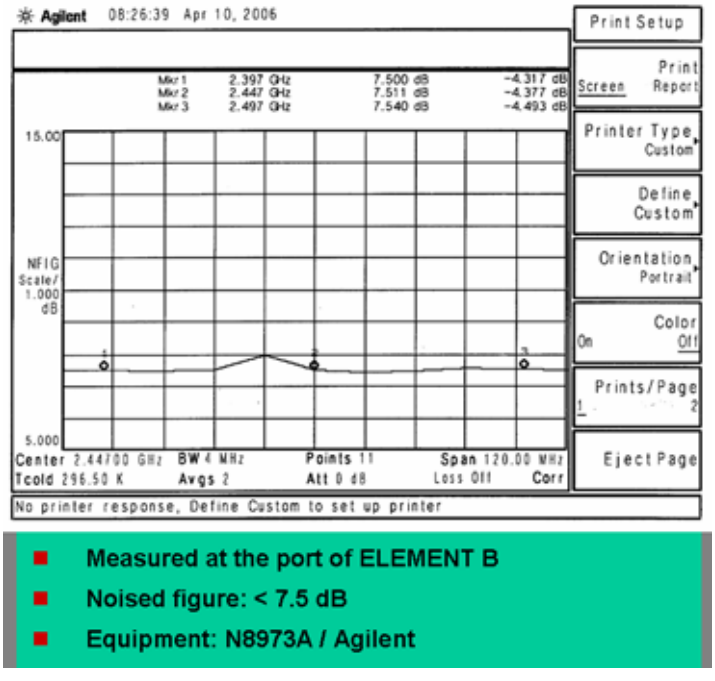

Graph 4-11 measured noise figure of OBU – ELEMENT B

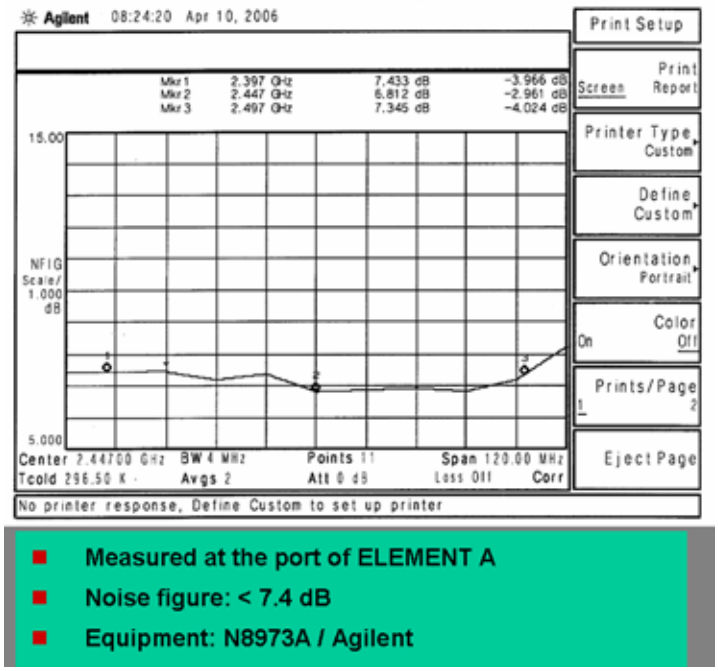

Graph 4-12 Measured noise figure of OBU – ELEMENT A

The summarization of basic electrical performances of RSU and OBU does be described in Figure 4-4.

	RSU	OBU
DC supply feed	10 Voltage / 1.1 Ampere (Max.)	10 Voltage / 1 Ampere (Max.)
TX output power (dBm)	5 dBm from 31.647 to 32.703 GHz	1 dBm from 37.497 to 38.553 GHz
TX conversion gain (dB)	5 dB / IF input power of 0 dBm	1 dB / IF input power of 0 dBm
RX conversion gain (dB)	-2 dB / injected RF band from 37.497 to 38.553 GHz with I/P power of -20 dBm	2 dB / injected RF band from 31.647 to 32.703 GHz with I/P power of -20 dBm
RX noise figure (dB)	< 9.8 dB, measured on N8973A / Agilent	< 7.5 dB, measured on N8973A / Agilent

Figure 4-4 the summarization of basic electrical performances of RSU and OBU

4.4 Link test

Graph 4-13 is the test setup of the link test. The linking process between elements on RSU and

elements on OBU is set to the Ad Hoc mode of IEEE 802.11 g communication protocol by the WLAN cards connected to note books.

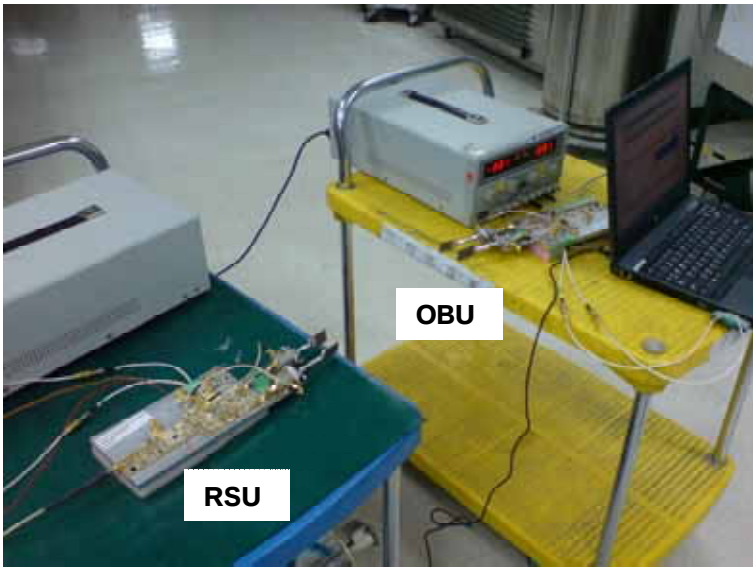

Graph 4-13 the test setup of the link test

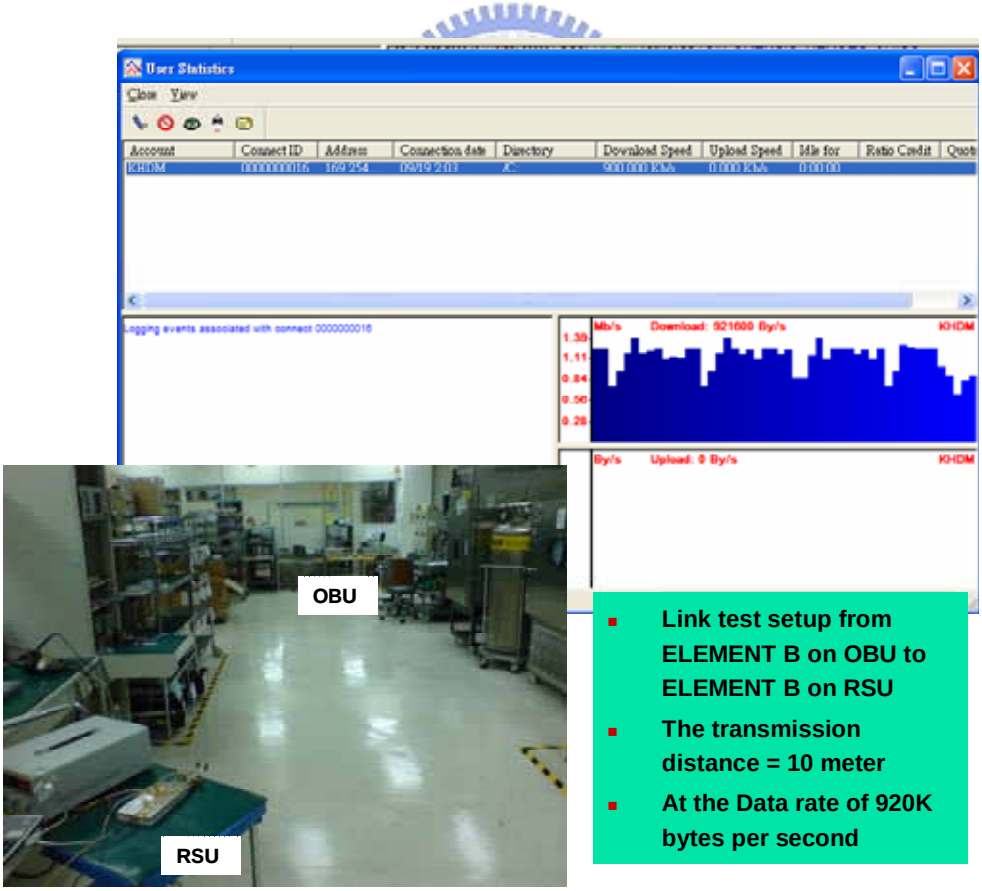

Graph 4-14 the link test from ELEMENT B on OBU to ELEMET B on RSU

Graph 4-14 is the link test form ELEMENT B on OBU to ELEMNT B on RSU under the

condition that the distance between them is 10 meter. The transmission data rate shown on the FTP software is 920K bytes per second.

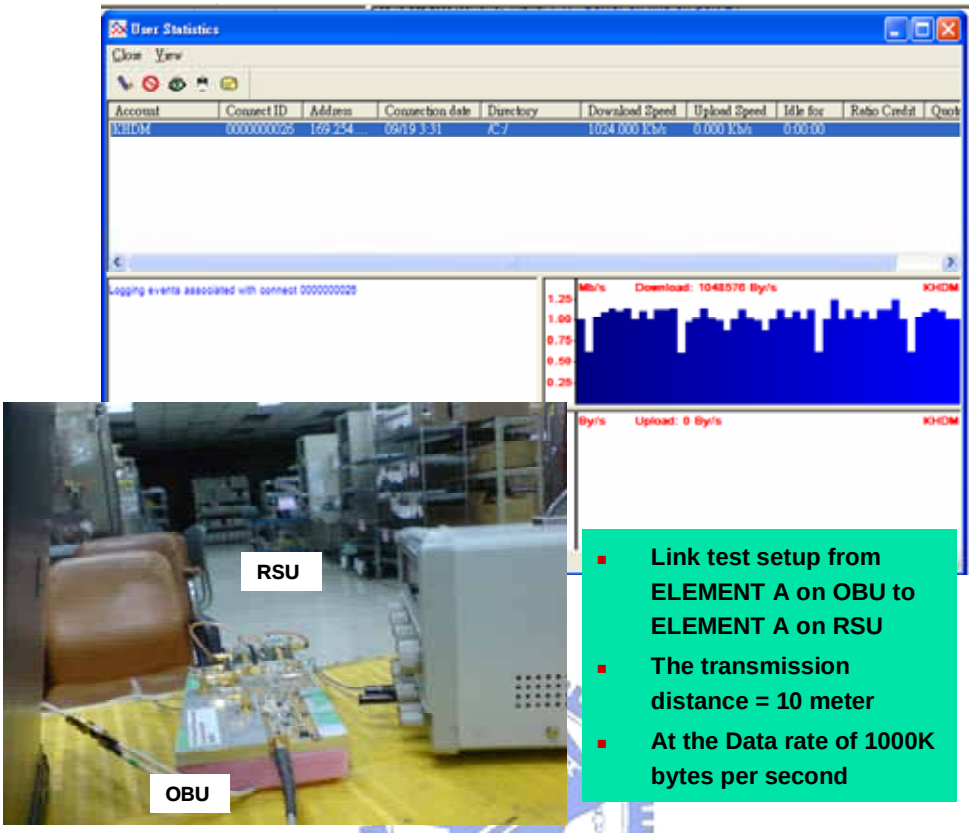

Graph 4-15 the link test from ELEMENT A on OBU to ELEMET A on RSU

Graph 4-15 is the link test form ELEMENT A on OBU to ELEMNT A on RSU under the condition that the distance between them is 10 meter. The transmission data rate shown on the FTP software is 1000K bytes per second.

CHAPTER 5 CONCLUSION

In this thesis, regarding to the convenience of the link test setup and measuring, two evaluated units as referred to RSU and OBU have been designed and manufactured to meet the requirement of dual services and the application of IEEE 802.11 b or g wireless communication.

The link distance between connected 802.11 g WLAN modules is measured ten meter under the average transmission data rate of 950K bytes per second.

By the arrangement for the frequency plan of ELEMENT A and B, the provided dual services would be for not only two 802.11 b or g WLAN module, but also other communication platform with different radio access methods, i.e.,

- WiMAX (Worldwide Interoperability for Microwave Access)

- GPS (Global Positioning System)

- VICS (Vehicle Information and Communication Systems)

- ETC (Electrical Toll Collection)

- DBS (Directly Broadcast Satellite)

- Integrated mobile communication for the application in the long tunnel: EUR GSM (Global System for Mobile communication), PHS (Personal Handy-phone System), US Cellular/PCS, GPRS (Global Packet Radio Service)

, and so on.

However, to fulfill the requisition of multiple services communication, the design of the multiplexing component and sub-circuitries for the element isolation in the IF sub-module will become more complicated and so will be the considerations of frequency plan and spacing between each element regarding to the local frequency sub-module.

Thus, for the available RF carrier-frequency band width and the ratio of cost to performance, the quantity of element provided by a Ka band HUB diplexer, in this paper, is better not greater than three.

REFERENCE

[1] Satoru SHIMIZU, Kinya ASANO, Kiyohito TOKUDA, “Special edition on ITS: Development of and ROF road-vehicle communication system”, OKI technical review 187 Vol. 68, Page(s):8-10, September 2001

[2] Sato, K.; Fujise M.; Shimizu, S.; Ikeda, H., “Propagation study of ITS multiple services road-vehicle communication using ROF technology”, Microwave Conference 2000 Asia-Pacific, 3-6 Dec. 2000, Page(s):481-484

[3] David M. Pozer, Microwave Engineering, John Wiley & Sons Inc., 2005, Third edition, Page(s):536-576

[4] Marvin Cohn; James E. Degenford; Burton A. Newman, “Harmonic Mixing with an Antiparallel Diode Pair”, IEEE Transactions on Microwave Theory and Techniques, Vol. MTT-23, NO. 8, Page(s):667-672, August 1975

[5] Jia-Shen G. Hong and M. J. Lancaster, Microstrip Filters for RF/Microwave Application, John Wiley & Sons Inc., 2001, Page(s):129-272

[6] O. P. Cutpa and R. J. Menzel, “Design tables for a class of optimum microwave band stop filters,” IEEE Trans., MTT-18, July 1970, 402-404

[7] F. Rasa; F. Celestino; M. Remonti; B. Gabbrielli; P. Quentin,“37-40GHz MMIC Sub-Harmonically Pumped Image Rejection Diode Mixer”, United Monolithic Semiconductor, the application note